The influence of restraint on the expansion of concrete due to delayed ettringite formation

Yuichiro Kawabata, Naoshi Ueda, Taito Miura, Stéphane Multon

The influence of restraint on the expansion of concrete due to delayed ettringite formation

Yuichiro Kawabata[1,*], Naoshi Ueda[2], Taito Miura[3] and Stephane Multon[4]

[1] Port and Airport Research Institute, 3-1-1, Yokosuka 239-0826, Japan

[2] Department of Civil, Environmental and Applied Systems Engineering, Kansai University, 3-3-35, Yamate-cho, Suita, Osaka, 564-8680, Japan

[3] Department of Civil Engineering, Nagoya University, Furo-cho, Chikusa-ku, Nagoya, Aichi, 464-8603, Japan

[4] LMDC, Université de Toulouse, INSA/UPS Génie Civil, 135 Avenue de Rangueil, 31077 Toulouse cedex 04, France

* Corresponding author: Yuichiro Kawabata

Tel.: +81-46-844-5059

Fax: +81-46-844-0255

Address: 3-1-1, Nagase, Yokosuka 239-0826, Japan

E-mail: kawabata-y@p.mpat.go.jp

Abstract

The influence of restraint on expansion, expansive pressure, and cracking patterns due to delayed ettringite formation (DEF) in concrete was experimentally evaluated. Especially, the expansive pressure was estimated with two approaches: calculation from the strain of the steel and direct measurement using load cells. The expansive behaviors were strongly affected by the restraint, especially in the restraint direction. The expansive pressure measured by the load cell was 1.9–3.9 MPa, which is nearly consistent with those calculated from the steel bar strain. The expansive pressure of DEF was almost the same order of magnitude as for ASR expansion, despite larger free DEF expansion than ASR. From a simplified calculation, it is estimated that the imposed DEF expansion was reduced from the stress-free expansion by approximately 80%. Although the total length of surface cracking was independent of the degree of the restraint, the distribution of surface cracks was significantly modified by the degree of the restraint. On the contrary, the inner crack pattern was similar for the restraint case while large gap formation was observed for the stress-free case.

1. Introduction

Delayed ettringite formation (DEF) is a concrete pathology that shows deleterious expansion of the order of several percent or more in the laboratory, leading to the cracking of concrete and causing crucial concern in the unexpected deformation or decrease in the integrity of the structures. As an alkali-silica reaction (ASR), DEF is recognized as an internal swelling reaction in concrete. DEF expansion is usually more serious than ASR expansion when considering the magnitude of expansion. While significant effort has been carried out to elucidate the microscope mechanism for DEF expansion (e.g., [1–3]), fewer studies on structural models are available [4–6]. To assess the performance of structures affected by DEF, it is important to understand the effect of stress on DEF expansion. In particular, the extent of the expansive pressure of DEF on concrete and how much stress is necessary to prevent DEF expansion. While there are fewer studies on such topics, the effect of restraint on DEF expansion is known to have critical differences from ASR expansion [7–8].

At the stress-free condition, DEF expansion can be considered as isotropic whereas ASR shows intrinsic anisotropy, which may be possibly due to the casting direction [9]. In the case of ASR under stress, the presence of steel reinforcement as well as active stresses such as prestressing reduces expansion in the restrained and loading directions [10–22]. According to Multon and Toutlemonde [13], the expansion is transferred to the direction with lesser compression, resulting in nearly equal volumetric expansion. Although it remains controversial whether such transfer is always observed for every concrete (e.g. [14]), "expansion transfer" is one of the key features of ASR expansion under stress. In contrast, for DEF mortar/concrete, while the expansion in the restrained or loading direction is reduced, the expansion in the transverse direction without any restraint is almost equivalent to free expansion [7–8], suggestive of a lack of expansion transfer. This leads to a reduction in the volumetric expansion of concrete for uni-axially restrained mortar/concrete (20–33% [7–8]). In particular, when concrete is triaxially reinforced, volumetric expansion is drastically reduced to 54% of that of free expansion [8].

While several studies on expansive pressure of ASR mortar/concrete have been reported [15–16, 23–26], to the knowledge of the authors, no studies on measuring expansion stress directly have been reported for the expansive pressure of DEF concrete. For ASR concrete, the expansive pressure of concrete due to ASR is significantly influenced by many factors, such as the reactivity of the aggregate and the total alkali content, and ranges from 0.1 to 6 MPa [15–16, 23]. The experimental conditions of three studies on expansive pressure are summarized in Table 1: two DEF experiments and one experiment on external sulfate attack (ESA) [27]. Bouzabata et al. [7] considered mortar bar restrained by four threaded stainless steel bars with different diameters corresponding to reinforcement ratios (*As*/*Ac*) of 0.8% and 4.9%. Based on the concrete strain at unloading, these investigators reported compressive stresses at the final expansion of 1.6 and 4.2 MPa for 0.8% and 4.9% *As*/*Ac*, respectively. By applying 14.5 MPa of compressive stress on the DEF concrete, Thiebaut et al. found that creep exceeds DEF expansion, leading to contraction of the concrete in the longitudinal direction [8]. Similar to DEF expansion, the expansive pressure of mortar due to ettringite formation subjected to ESA was measured by Müllauer et al. Thin-walled mortar cylinders were restrained by an inner stainless steel tension bar and the end-plate disk, and were exposed to sodium sulfate solutions [27]. The resulting expansive pressure reached around 8 MPa, which is significantly higher than the tensile strength of mortar.

In terms of cracking, both surface and internal cracking must be considered, with the cracking reducing the mechanical properties of the concrete. For surface cracking, DEF concrete subjected to uni-axial restraint exhibits oriented cracking along the direction of the restraint, while map cracking is observed for stress-free DEF concrete [8]. This tendency is similar to ASR, where uni-axial stress modifies the orientation of the micro-cracks, which may cause an anisotropic modification of the mechanical properties [14, 22, 28]. At the microstructural scale, when DEF expansion occurs without external stress, cracks are formed in the cement paste and around aggregates. However, it is unknown whether the orientation of gaps or microcracks can be modified for DEF under stress.

Consequently, there have been fewer studies on structural/mechanical models of concrete affected by DEF expansion than studies on ASR. In particular, understanding effect of varying degrees of restraint on DEF expansion and damage (i.e., cracking patterns) is important for assessing the structural behavior of reinforced concrete. In the present study, experiments with different degrees of restraint are carried out to evaluate the expansive pressure of concrete due to DEF expansion, with two approaches adopted: calculation from the strain of the steel and direct measurement using load cells. The expansive pressures from these approaches are compared in addition to the cracking patterns of concrete with varying degrees of restraint, which is important for assessing the mechanical response of concrete damaged by DEF.

2. Experiments

2.1 Test specimens

Three concrete specimens per case, restrained by steel round bars with different diameters (9.2, 13, 17, and 26 mm in diameter) were prepared. For one of the three specimens for each case, a load cell was installed to measure the expansive pressure of the concrete. Hereafter, specimens and their corresponding case are denoted by the diameter of the steel bar, e.g., "ϕ 9.2". The preparation of the test specimen is described in the following.

The mixture proportion of the concrete is provided in Table 2. The chemical composition of the high-early-strength Portland cement (Type III Portland Cement) used is shown in Table 3. The mineral composition by Bogue equation is shown in Table 4. A portion of the cement was replaced by K_2SO_4 reagent so that the total SO_3 content was increased to 5.6% of the cement by weight, with the K_2SO_4 reagent added to the mixing water in advance. Non-reactive sand and gravel were used for aggregate. The water-to-cement ratio (including K_2SO_4) was 0.49.

The apparatus for the test including a concrete specimen is shown in Figure 1. The specimens were cast in a 100×100×340 mm prismatic mold, which had a PVC pipe with an outer and inner diameter of 38 and 32 mm, respectively, placed at the center. Early-age curing was started four hours after the initiation of the mixing step, following a curing cycle of heating to 90 °C at a rate of +46.7 °C/h, maintaining for 12 h, and then cooling to 20 °C at a rate of -7 °C/h. Following early-age curing, the concrete specimens were demolded and the PVC pipe removed. The concrete specimens were wrapped with plastic film at 20 °C and cured until 28 days. Thereafter, 30-mm thick steel plates with a 38-mm diameter at their center were placed at the longitudinal ends of the concrete specimens. In these plates, a small hole was provided to allow the cable of the strain gauge to drain. Additional 6-mm thick steel plates were added, and a hole in these plates was made to match the diameter of the steel bar. For a single specimen for each case, a load cell (maximum capacity of 300 kN) was installed to measure the expansive pressure. A steel bar was inserted through the hole of the specimen and a small pressure (around 0.1 MPa) applied by tightening the nuts so that the concrete specimen, the steel bar, and the steel plates were fixed. Two strain gauges (gauge length of 2 mm) were attached to the surface of the steel bars to monitor their strain. Furthermore, no grouting was applied in the hole so that no bond stress developed between the concrete and the steel bar. As a typical example, the case with a 17-mm diameter steel bar is shown in Figure 1. For comparison, a 100×100×400 mm prismatic specimen without the hole was prepared for stress-free expansion.

The compressive strength and Young's modulus for a cylindrical concrete specimen with a diameter of 100 mm and a length of 200 mm was 32.3 MPa and 28.6 GPa, respectively, before the test (28 days). After the test, when the expansion was 2.17%, the strength and modulus had decreased to 6.8 MPa and 1.2 GPa, respectively.

2.2 Expansion test

After assembling the restraint apparatus with the concrete specimens at 28 days, the specimens were immersed in water. To prevent corrosion of the steel plates and steel bars, they were connected with magnesium alloy as a sacrificial anode. The water was replaced for each measurement. The test continued until 181 days after the test initiation, when the free expansion had almost reached a plateau.

The concrete expansion was measured on the surface of the concrete. The locations of the measurement points are shown in Figure 2. The concrete specimens were supported on the L-shaped stainless steel plates and the span was 250 mm during storage and measurement. In Figure 2, the green points indicate the location of the studs for measuring the longitudinal expansion while the blue points are similarly the locations for the lateral expansion. The change in the length of the concrete specimens was measured using a dial gauge for the longitudinal direction and a micrometer for the lateral direction, each with precisions of 0.001 mm. The expansion was then calculated by dividing the change in length by the gauge length. The initial length was measured before the test (28 days). The longitudinal expansion was monitored from the beginning of the test, and measurements of the lateral expansion began after longitudinal expansion began (70 days after the beginning of the test). The measurement length of the longitudinal and lateral expansion was 300 and 100 mm, respectively. Measurements taken at two and three locations for longitudinal and lateral expansion, respectively, for each test specimen. Strains of the steel bar and expansive pressure were monitored with a data logger. The strain and pressure were zeroed after specimen insertion in the container filled with water.

2.3 Crack observation

Surface cracking was observed after 181 days. Cracks were traced by illustration software and the raster data was converted to vector data. The length and the orientation of the surface cracks were then analyzed.

Afterward, one of the three concrete specimens was cut at the center in the longitudinal direction, and then half of the specimen was cut longitudinally (100×170 mm). The other half of the specimen was cut at a thickness of 30 mm perpendicular to the longitudinal direction.

The cut samples were impregnated under vacuum with low viscosity fluorescent epoxy resin with a small amount of ethanol to reduce the viscosity. Subsequently, after releasing the vacuum, 0.3 MPa additional atmospheric pressure was applied to the sample for thirty minutes. After the resin had hardened sufficiently, the surface of the concrete was roughly ground. Finally, the surface of the concrete was observed under ultraviolet light. Note that these conventional processes might induce microcracks or small damage to the specimens whilst comparison between the cases can be possible.

3. Results

3.1 Expansion measured from the concrete surface

(1) Stress-free expansion

The expansions of the concrete specimens due to DEF in the longitudinal and transverse directions are illustrated in Figure 3, with the error bars denoting the standard deviations of the measured expansions. In Figure 3(a), in the stress-free condition, the onset of expansion was around 50 days and exceeded 1.5% at 97 days. The rate of expansion in this interval was around 0.025% per day. Above an expansion of 1.5%, the rate of expansion gradually reduced with an expansion of 2.0% reached at 139 days, with a rate of expansion of approximately 0.01%/day. After this time, the expansion begins to plateau. Similar tendencies can be seen for the cylindrical specimen, although its rate of expansion was slightly higher. The transverse stress-free expansion, shown in Figure 3(b), was nearly equal to the longitudinal expansion. The standard deviation of the longitudinal expansion for the prismatic specimen was smaller than the transverse expansion. This is due to the different gauge lengths, the gauge for the longitudinal direction being three times longer. Indeed, the longitudinal expansion of the cylindrical specimen (gauge length of 100 mm) demonstrated a relatively larger standard deviation. The longitudinal and transverse expansions showed similar expansive behavior after 70 days, indicative of an almost isotropic DEF expansion at the stress-free condition [9].

(2) Expansion under restraint

The expansive behaviors were strongly affected by the restraint, especially in the longitudinal direction, as shown in Figure 3(a). Furthermore, the degree of the restraint had a lesser impact on the longitudinal expansion. The final expansion of the restrained concrete ranged from 0.27% to 0.39%, corresponding to an 82–87% reduction from the free expansion. Although the asymptotic final expansion differed, the kinetics of the restrained expansion were nearly equivalent to that of the free expansion. This tendency is also reported by Bouzabata et al. for mortar [7]. The transverse expansion (Figure 3(b)) showed contradictory results to previous studies, which reported that the transverse expansion was nearly equal to free expansion [7–8]. In the present study, regardless of the degree of the restraint, the transverse expansion was considerably smaller than free expansion, with a reduction of 20–32%. One of the reasons for the reduction can be attributed to the restraint from the steel plates at the longitudinal end of the specimen (Figure 1): friction between the steel plates and the concrete specimen would influence the transverse expansion.

The expansive behaviors along the transverse direction at the center of the longitudinal direction (Point B) is shown in Figure 4(a) and the transverse expansions at different locations are summarized in Figure 4(b). The measurement points are illustrated in Figure 2. The expansion measured at the center of the longitudinal direction (Point B) was 30–41% larger than the those measured near the end of the longitudinal direction (Point A and C) and was 17–24% larger than the average expansion. The transverse expansions at the center (Point B) were 75–90% of the stress-free expansion (Figure 4(a)). Thiebaut et al. reported that the expansion of concrete uni-axially restrained by an internal reinforcement was around 90% of unrestrained concrete in the transverse “stress-free” direction [8]. Additionally, Bouzabata et al. showed that the expansion of mortar in the stress-free direction was not modified [7]. In the present experiment, the reduction of the transverse expansions was relatively larger than in these previous experiments. Therefore, the influence of the restraint from the friction of the steel plates on the transverse expansion would be slightly larger in this study.

For further information, the expansive behavior of the concrete after releasing the restraint is summarized in Appendix 1.

3.2 Steel strain

The following process was performed to compare the steel and concrete strain. It should be noted that the 340-mm long concrete specimen was restrained by two steel plates. The length of steel between the plates was 416 mm in length without the load cell and 516 mm with the load cell. The difference in length was due to the presence of the steel plates and washers ((t30 mm + t6 mm + t2 mm)×2). As the displacement at the extremity of the concrete and steel was equal, the compatibility of the steel deformation should be maintained when compared with the concrete strain. Therefore, to be able to compare concrete and steel strains, the strain on the steel bar was reevaluated as follows (Figure 5). The deformation of the steel bar is the multiplication of the length of the steel bar between the nuts with its strain, given as

$$\delta_{\mathrm{bar}}=L_{\mathrm{bar}}\varepsilon_{\mathrm{bar}}, \tag{1}$$

where δ_{bar} is the displacement at the extremity of the steel bar (mm), L_{bar} is the restrained length between the nuts (L_{bar} = 416 mm without the load cell, L_s = 516 mm with the load cell), and $\varepsilon_{\mathrm{bar}}$ is the measured strain of the steel.

The deformation of the concrete is also given by

$$\delta_{\mathrm{con}}=L_{\mathrm{con}}\varepsilon_{\mathrm{con}}, \tag{2}$$

where δ_{con} is the displacement at the extremity of the concrete (mm), L_{con} is the length of the concrete prism (L_{con} = 340 mm), and $\varepsilon_{\mathrm{con}}$ is the measured strain on the concrete surface.

Assuming that the deformation of the steel plates is negligible, the displacements at the ends of the concrete and steel bar should be equal ($\delta_{\mathrm{bar}}=\delta_{\mathrm{con}}$), giving

$$\varepsilon_{bar}=\frac{L_{con}}{L_{bar}}\varepsilon_{con}. \tag{3}$$

Therefore, the steel bar strain with and without the load cell is 82% and 66% of the concrete expansion strain, respectively. Therefore, the measured strain of the steel bar was reduced to these values.

The behavior of the calibrated steel bar strain is shown in Figure 6. Due to low insulation resistance, the strain data for the ϕ 13 case was not available after 95 days. In all cases, the steel strains increased linearly from around 50 days and showed a convergent trend after approximately 100 days. The final strain of the steel at 181 days was 1537 μm/m for ϕ 9.2 and decreased with increasing diameter of the steel bar (ϕ 17: 744 μm/m, ϕ 26: 403 μm/m).

3.3 Expansive pressure

The load cells allowed direct measurements of the restraint stresses in the concrete specimens. The restraint stress represents a macroscopic evaluation of the expansive pressure. The changing pressure with time as obtained by the load cells is shown in Figure 7. The expansive pressure increases with increasing concrete expansion and steel strain. For ϕ 26, although a small compressive stress was induced initially, a small drift was measured at approximately 50 days. Note that such a drift could not be observed for the steel strain. This drift might have reduced the measured expansive pressure.

3.4 Cracking patterns

The surface crack patterns of the concrete specimens after the test are shown in Figure 8. Map cracking is observed for the stress-free expansion, with a maximum crack width of 2 mm. For the restrained specimens, the cracking patterns were somewhat consistent, with clear cracks along the longitudinal direction that were filled with white deposits. The larger the degree of the restraint, the larger the crack width and the fewer the number of cracks in the longitudinal direction. Relatively large cracks extended in the longitudinal direction, and smaller cracks extended in the transverse direction as well. As the degree of the restraint increased, the small cracks extending along the transverse direction became less than those observed for the stress-free expansion. The maximum crack width at the surface was almost equal (0.4 mm) for the four restraint cases, independent of the diameter of the steel bar, and significantly lower than for the stress-free specimen (0.4 versus 2 mm for the stress-free expansion). The total crack length and crack orientation are shown in Figure 9. The crack orientation was defined as the angle from the transverse direction (cracks with an angle of 90° are along the longitudinal direction). The total crack length was around 800-1100 mm for all the specimens, and thus had no correlation with the degree of restraint. The work by Kchakech reported that there is a correlation between stress-free expansion and the total crack length and that the first visible cracks coincided with the inflection point of the expansion curve [29]. In this study, although the kinetic behavior of surface cracking was not evaluated, Figure 9(a) indicates that the kinetic relation between expansion and the total crack length under restraint is different from stress-free one. In contrast, the crack orientation was strongly influenced by the degree of constraint: the unrestrained specimen demonstrated perfectly isotropic cracking with very few dispersions along all directions, and specimens with the largest restraint (φ17 and φ26) exhibited more than half their cracks in the 60-90° direction. This demonstrates a key anisotropy in the cracking even if cracks in all directions can be observed.

The inner crack pattern of the concrete specimen after the test in the transverse and longitudinal directions is shown in Figure 10 and Figure 11, respectively. In the figures, the area where the concrete surface is uneven due to aggregate debonding is encircled by red dotted lines; since the concrete was heavily damaged by DEF expansion, it was difficult to cut the specimens without inducing any damage. The fluorescence can be observed for all cases, especially around the coarse aggregate, which is generally termed as a "gap". The gaps are opening providing evidence of DEF expansion. The fluorescence was also observed in pores and cracks. The width of the gap is the largest for the stress-free specimen for both directions. For the restrained specimens, no distinct difference could be found. It is known that the gap forms as a result of expansion and is related to the magnitude of expansion: the larger the expansion, the larger the width of the gap [30]. The trends in the inner crack pattern seem consistent with the results of the expansion test. At the surface, fine cracks in the transverse direction were reduced according to their degree of restraint. It should be noted, however, that the cracking patterns for ϕ 17 and ϕ 26 did not change significantly. For internal cracks, no clear difference with varying degree of restraint was observed for gaps and cracks, although there is a considerable difference between the restrained specimens and the stress-free expansion. As for stress-free specimens, the maximum width around the coarse aggregate reached 1.0 mm. It could be hypothesized that such a large width might be attributable to the opening during the operations performed for the observation such as cutting and impregnation; but this was confirmed to be of the same order of magnitude by nondestructive x-ray micro computed tomography (CT) on a cylinder specimen with almost the same expansion (0.9 mm in width for an expansion of 2.17%, see Appendix 2), suggesting that the width of 1.0 mm is attributed to DEF expansion. The width around the coarse aggregate is reduced to approximately 300 μm for the restrained specimens. For the width of the gap across the cross-section along the longitudinal and transverse directions, no apparent tendency between the specimens can be found.

4. Discussion

4.1 Anisotropy of restrained DEF expansion

The relationship between longitudinal and transverse expansion is illustrated in Figure 12. As described above, the stress-free expansion demonstrated nearly isotropic behavior while the stressed concrete demonstrated strong anisotropy. In each case, there is a quasi-linear relationship between the longitudinal and transverse expansions. Anisotropic coefficients (longitudinal /transverse expansion) calculated from the average expansions are within 0.14–0.22 for the restrained specimens, similar to the results of previous studies [7–8]. Note that the anisotropic coefficients are within 0.09–0.19 when the transverse expansion at Point B was used for calculation. The anisotropy of the expansion is confirmed by the quantification of the orientation of the induced cracks (Figure 10).

To compare the results with those of previous studies [7–8], the ratio of the cross-sectional area of the steel bar and the concrete, *As*/*Ac*, was calculated. Figure 13 shows the “expansion ratio” versus *As*/*Ac*, where the expansion ratio is defined by the decrease of longitudinal expansion due to the steel restraint (ratio of the expansion of the restrained concrete to the stress-free expansion). For comparison, results for ASR expansion from the literature are also shown in the figure [16, 21]. Note that, for the data from Mohammed et al., only the cases with end plates are plotted as expansions measured on specimens without steel plates can be affected by the loss of a portion of the steel-concrete bonding for high degrees of expansion. The expansion ratio is greatly influenced by *As*/*Ac*, irrespective of the cause of expansion (ASR or DEF). Only a small *As*/*Ac* ratio, and thus a small restraint rigidity, drastically changes the expansion in the restrained direction, while the degree of restraint has a minor impact when *As*/*Ac* is over 1.0%. Although results for the restrained cases with *As*/*Ac* below 0.5 is not available for DEF, the general trend for the reduction in longitudinal expansion due to the restrained expansion as measured for the mortars and concrete seems to be similar between DEF and ASR. The relationship between *As*/*Ac* and anisotropy coefficients is summarized in Figure 14. Although the chemical mechanisms of expansion are completely different between ASR and DEF, the mechanical response of concrete to these two types of internal expansion seems similar. Since the expansion transfer cannot be found for DEF as for ASR (Figure 3, 12), the influence of the restraint on the expansion along the restrained direction is larger for DEF. Thus, a similar quantitative trend to the expansion ratio can be found: even a small degree of restraint can greatly reduce the anisotropic coefficient. The anisotropic coefficient does not reach zero even when the concrete is highly restrained; the minimal ratio of approximately 0.2 corresponds to the longitudinal expansion necessary to obtain a sufficient longitudinal compressive stress to arrest expansion along this direction. The results in this study are consistent with those of previous studies on mortar and concrete submitted to DEF and ASR [7–8, 16]. These results also increase the domain of validity for the evolutions of the expansion and anisotropy ratios in the case of concrete reinforced by high steel ratios and submitted to DEF.

4.2 Expansive pressure

The strains measured on the steel bars can be used to evaluate the expansive pressure and thus be compared to the direct measurement of pressure from the load cell. First, the expansive pressure was calculated from the steel strain as shown in Figure 15. Note that the raw data of the steel bar strain was used "without calibration" for the pressure calculation since the stress induced by the steel bar is reflected by the actual strain of the steel bar. Additionally, the relationship between the load-cell measurement and the calculation is summarized in Figure 16. The trend in the calculation results is consistent with the measurement (± 0.25 MPa) except for the ϕ 26 case. In this case, above 0.5 MPa of measured pressure, the measurement is around 65% of the calculated pressure. While the steel was located in the center of the concrete and the average expansion of the concrete was measured, the load cell requires a uniform stress acting on the bearing area of the load cell. However, DEF expansion is not uniform across the cross-section, and thus the eccentric stress deriving from the difference of expansion across the cross-section might affect the measurement results of the load cell. This may have possibly occurred due to the presence of the small interspace or the deformation of the steel plates. Such a loss of expansive pressure may have occurred for the ϕ 17 case, where slip-like behavior was observed at 2.0 MPa. However, it should be noted that the slope before and after the slip is equal so the lost pressure seems to be small (possibly 0.5 MPa).

Furthermore, assuming compatibility between the concrete (ε_c) and steel (ε_s) strains, the expansive pressure can be calculated from the expansion strain of the concrete. As a result, the expansive pressure calculated from the concrete strain and the Young's modulus of the steel bar ranges from 5.7 to 20.7 MPa, which is unrealistic as compared to previous studies [7–8]. The unrealistic evaluation of pressure from the concrete strain may result from structural deformation during expansion as discussed in the following section. Actually, according to the experiment by Thiebaut et al., 14.5 MPa of applied compressive stress contracts the concrete without any expansion [8]. A summary of *As*/*Ac* versus expansive pressure, including the results of previous studies [7–8], is illustrated in Figure 17. Complementary results for DEF under bi-axial restraint are presented in Appendix 3. These results are not presented in the main body of this study as they were obtained for a different concrete under different environmental conditions; however, they can provide interesting insight on multi-axial restraint, particularly in terms of expansive pressure. In the present study, the expansive pressures measured by the load cell and calculated from the steel strain are generally consistent. At an *As*/*Ac* of 6.0, the expansive pressure measured by the load cell is lower than the calculated pressure due to the afore-described mechanism. The results of Thiebaut et al. show the greatest expansive pressure as calculated from the concrete surface expansion despite a lower *As*/*Ac*. However, the data of Thiebaut et al. is within the range of the expansive pressure resulting from external sulfate attack [27]. It should also be noted that, in the experiment by Thiebaut et al. [8], the steel bar was embedded in concrete, while in the present study and the experiment by Bouzabata, an external restraint system was used without bonding, so the effect of bonding between concrete and the steel bar might have an impact.

As for the ASR expansion of concrete under stress as measured by Kagimoto et al., the expansive pressure for different degrees of restraint ranged from 0.3 to 2.6 MPa [16]. Additionally, for the experiment by Berra et al., the expansive pressure of concrete was measured for different mixes and initial stresses, with a single restraint condition considered [15]. As a result, the expansive pressure was between 0.45-5.6 MPa (for concrete with stress-free expansion between 0.04 and 0.5%). As for the mortar with two different aggregates, Kawamura and Iwahori measured expansive pressures between 0.4 and 4.5 MPa [23]. The relationship between the expansive pressure obtained for expansion under restraint conditions and the unrestrained ultimate expansion is summarized in Figure 18, including the case of ASR with DEF data. No obvious tendency can be found, which may be due to the differences of restraint levels between experiments. However, the level of macroscopic pressure obtained for DEF and ASR under restraint conditions is below 6 MPa for free swelling until 2.5%, regardless of the origin of expansion. Comparing the expansive pressure from ASR and DEF, it is notable that the expansive pressure is almost on the same order of magnitude as the ASR pressure, ranging from 0.3 to 6 MPa, despite a larger free DEF expansion as compared to ASR. The stress-free expansion due to DEF is one order of magnitude greater than that of ASR. Nevertheless, it is possible that a small degree of restraint is sufficient to reduce DEF expansion. In laboratory experiments, As/Ac is generally higher than that of real structures, and thus more investigations will be necessary. However, it should be noted that the expansion cannot be perfectly prevented by the passive restraint as sufficient expansion is needed to induce significant compressive stresses. Active application of a compressive stress such as prestressing may be necessary to prevent any expansion.

4.3 Steel and concrete strains

The relationship between the expansion of the concrete surface and the steel strain is shown in Figure 19. Here, the strain of the steel bar is calibrated according to Eq. (1) – (3). The strain measured on the steel bar was not equal to the expansion strain measured on the external surface of concrete. The ratio of the steel strain to the expansion strain of the concrete at the end of the test was the highest for ϕ 9.2 (42%) and the lowest for ϕ 26 (14%). There may be several reasons for the discrepancy between the concrete expansion and steel strain. The first consideration is the rigidity of the load cell. In the discussion between Kagimoto and Hansen [31–32], the stiffness of the testing apparatus has a critical impact on the expansive pressure as experimentally measured for ASR. This is also the case for DEF expansion. To evaluate the impact of the load cell on the steel strain, all deformation mechanisms were evaluated:

- the deformation of load cell at 30 kN of compression (corresponding to 3.4 MPa of expansive pressure) is theoretically 0.009 mm.
- the steel plates were deformed by compression, which should be approximately 0.001 mm.

For instance, as for the ϕ 9.2 case, considering the final length after 0.15% expansion, the deformation of the steel bar is 0.63 mm. Therefore, the longitudinal deformation of the restraint apparatus after final expansion is 0.62 mm (0.062 = 0.63 - 0.009 - 0.001 mm). The expansion of the concrete calculated from the deformation of the restraint system would be 0.18%, which is around half that of the measured expansion at the concrete surface.

Second, there may be possible corrosion of the steel plates. This corrosion would be almost negligible since the steel plates and steel bar were protected by sacrificial anodes (Mg alloy) and visible corrosion could not be found after the test. Finally, there is the mechanical instability of concrete specimens with holes inside them. The minimum thickness of the concrete is 31 mm. Compared to massive specimens such as those used in the experiment performed by Thiebaut et al. [8], the specimen might deform and become barrel shaped. In this case, the steel strain could be smaller than the expansion strain of the concrete surface, as concrete shows considerable out-of-plane deformation. For instance, according to the experiment by Müllauer et al. [27], in which a stainless steel bar was embedded in a thin-walled mortar specimen, some of the mortar specimen showed buckling damage. Although visible buckling could not be observed in Figure 8–11, this mechanism may explain why the ratio of the steel strain to the expansion strain of the concrete decreases with increasing steel bar diameter. When the diameter of the steel bar increases, the compressive stress acting on the concrete specimen is higher, resulting in pronounced out-of-plane deformation despite the small expansion. Consequently, a smaller steel strain is obtained in the highly reinforced specimen.

Many studies have assumed perfect bonding between steel and expansive concrete. However, typically, the expansion strain is only measured on the external surfaces of the concrete. Few experimental works have compared the external concrete strain and the reinforcement steel strain measurements as in the present study and no possible comparison is available. The choice of a specimen with a hole may have led to structural buckling and thus resulted in the difference in the strains measured on concrete and steel in the present study. To improve this analysis, future numerical analyses are planned to model the present experimentation with a mesoscale modeling [33].

4.4 Reduction in expansion in the presence of the restraint

Considerable reduction in longitudinal expansion was found in the presence of the restraint. There may be two possible primary mechanisms: the reduced expansive potential of DEF and enhanced creep strain. In this study, the expansive potential of DEF as modified by the restraint is focused on. The relationship between imposed DEF expansion and restrained expansion may be given by Eq. (4), with tension (expansion) defined as positive:

$$\varepsilon_{res}=\varepsilon_{e}+\varepsilon_{cr}+\varepsilon_{imp}, \tag{4}$$

where ε_{imp} is imposed DEF expansion, ε_{e} is the elastic strain from compression (induced by the restraint), ε_{cr} is the creep strain under restraint, and ε_{res} is the expansion strain under restraint. The strain measured before and after releasing the restraint is considered as elastic strain (ε_{e}). In this case, the Young's modulus can be calculated from the expansive pressure measured by the load cell (σ_{DEF}) and the differential elastic strain (ε_{e}) between before and after releasing the restraint. Note that the Young's modulus was measured from stress-free cylindrical specimens (see Section 2.1, E_{c} = 1.2 GPa). The creep strain can be calculated assuming that the creep coefficient ($\varepsilon_{cr}/\varepsilon_{e}$) is constant at 2 regardless of the expansion.

The calculated result is shown in Table 4. From the calculation, the imposed DEF expansion was reduced from the stress-free expansion by approximately 80%. The estimated Young's modulus is seven to nine times higher than that of the stress-free specimen after the test. It is notable that DEF expansion under restraint is reduced significantly. In this calculation, creep was assumed to be not modified by DEF. Therefore, although it is difficult to conclude which mechanism is dominant for the reduction in DEF expansion under the restraint condition, an approach considering a reduction in DEF expansion under restraint may be possible for further modeling. Further research is required to quantify the relationship between stress and DEF expansion under stress. Besides, the results in this paper clearly indicated a possibility that a small degree of restraint is sufficient to reduce DEF expansion. Whilst this study showed the DEF expansion under uni-axial restraint (bi-axial restraint as well in Appendix), the effect of three-dimensional restraint on DEF expansion, which is more likely to be real structure, is also necessary to be investigated.

5. Conclusions

The influence of restraint on expansion, expansive pressure, and cracking patterns due to delayed ettringite formation (DEF) in concrete was experimentally evaluated and compared to a large number of experimental results on the effect of restraint on internal swelling reaction (ASR and DEF). The conclusions can be summarized as follows:

(1) Longitudinal expansion was considerably reduced (82–87%) in the presence of restraint while the reduction in the transverse expansion was 20–32%. The reduction in the transverse expansion might be attributable to the restraint provided by the steel plates at the end of the specimen. The decrease in longitudinal expansion was consistent with experimental results in the literature obtained for mortar. The present experimental results provide quantitative conclusions for concrete and for intermediate degrees of restraint.

(2) For the first time, expansion pressure was evaluated directly for DEF expansion under restraint. The pressure measured by the load cell was 1.9–3.9 MPa, which is nearly consistent with those calculated from the steel bar strain. The expansive pressure calculated from the strain of the concrete surface was significantly higher than those directly measured with the load cell, possibly due to out-of-plane deformation of the holed specimen. The expansive pressure of DEF was almost of the same order of magnitude as for ASR expansion, despite larger free DEF expansion than ASR.

(3) This experimental work leads to important results concerning the quantification of cracks on the surface and the observations of inner cracks in concrete specimens submitted to DEF under restraint:

a. The total length of surface cracking was independent of the degree of the restraint,
b. The orientation of cracks was isotropic for concrete subjected to DEF in stress-free expansion,
c. The anisotropy of cracks due to restrained DEF expansion was quantified in terms of the cracks distribution,
d. The inner crack pattern was similar for the restraint case while large gap formation was observed for the stress-free case.

The quantification of cracks of DEF-damaged concrete is an important issue for the management of affected structures as cracks affect the supply of water in the material and can accelerate the damage of concrete in combination with other external attacks.

Acknowledgements

Part of this work was financially supported by the Japan Society for the Promotion of Science (JSPS, No. 20H02227). The authors also would like to thank Dr. Badreddine Kchakech for providing advice on the crack pattern analysis.

Appendix 1: Expansive behavior of concrete after releasing the restraint

After 181 days, the apparatus for the restraint was removed from the concrete specimen. Then, using two specimens that were not used for crack observation, the expansion of the concrete specimen after stress release was continuously measured. The expansion curves of the concrete specimens after releasing the restraint are given in Figure A1. The longitudinal and transverse expansions gradually increased with time. No trend in the increased expansion after releasing the restraint can be observed. The trends seem to be similar for the four restraints.

The relationship between the longitudinal and transverse expansions is illustrated in Figure A2. In this figure, the expansion was normalized by subtracting the final expansion before releasing the restraint. As for the stress-free specimen, an almost isotropic expansion can be confirmed (a ratio of 1.14 between transverse and longitudinal expansions). In contrast, it was found that the curves for the stress-released specimens (formerly restrained specimens) are concave up when the longitudinal expansion is less than 0.15%, with the longitudinal expansions then mostly linear with transverse expansion. The larger longitudinal expansion below 0.15% longitudinal expansion might be attributable to elastic deformation and creep recovery after releasing the restraint. Above 0.15%, the ratios of the transverse expansions to the longitudinal expansions are 2.0-2.6 for the stress-released specimens, suggesting an anisotropic expansion of the concrete even after releasing stresses. This might be due to anisotropic damage induced during the restraint. In actual structures affected by DEF expansion, the stress states are complex, and thus care must be taken when performing an expansion test on concrete core extracted from an already-damaged structure: when only longitudinal expansion is measured, the potential residual expansion may be underestimated.

Appendix 2: Internal cracking pattern captured by x-ray microtomography scanning

A 100-mm in diameter cylindrical specimen 200 mm in length after the expansion test was used for nondestructive x-ray microtomography scanning (X-μCT). Expansion of the specimen after the test was 2.17%. The ScanXmate-D200RSS900 x-ray CT scanner system located at the Port and Airport Research Institute in Yokosuka, Japan, was used for the investigation. The maximum voltage and current of the x-ray tube are 225 kV and 0.6 mA, respectively. The transmitted x-rays are detected by a 418 by 418 mm flat panel with a resolution of 3008 by 3008 pixels.

The x-ray CT image of the concrete cylindrical specimen is shown in Figure A3. The gaps around the aggregate can be easily observed. The maximum width of the gap is estimated as 0.9 mm, which is consistent with the observation using fluorescent epoxy resin.

Appendix 3: Expansion of concrete under bi-axial restraint

To evaluate the expansive behavior of concrete under bi-axial restraint, the following experiments were carried out in Kansai University.

A3.1 Experiments

A3.1.1 Test specimens

Cylindrical concrete specimens surrounded by a stainless cylindrical tube with a 100-mm diameter, as shown in Figure A4, were used for DEF expansion test under bi-axial restraint. Three degrees of restraint were considered by changing the tube thicknesses. The thicknesses of the stainless tube were 0.25, 0.5, and 1.0 mm, giving restraint ratios along the circumferential direction of 0.5, 1.0, and 2.0%, respectively. Apart from the uni-axial restraint condition, the DEF concrete expansion in the circumferential direction was bi-axially restrained by the tube. In contrast, the longitudinal expansion was restrained by the friction between the concrete and the stainless tube. The concrete was actually subjected to tri-axial restraint; however, the degree of restraint in the longitudinal direction was lower, as shown in **A3.2.1**. Therefore, in this study, this experimental case is regarded as "bi-axial restraint". Hereafter, the specific test cases are denoted by the thickness of the stainless tube, e.g., "t0.25". Three cylinders were prepared for the stress-free, t0.5, and t1.0 specimens while two cylinders were prepared for the t0.25 specimens. The test specimen details are described as follows.

The mixture proportion of the concrete is shown in Table A1. The cement was Ordinary Portland Cement (Type I Portland Cement), which differs from the cement used for the samples in the main body of this study (see Table 2). The SO_3 content of the cement was 2.17%. A portion of the cement was replaced by a K_2SO_4 reagent so that the total SO_3 content was increased to 8.8% of the cement by weight. K_2SO_4. Non-reactive sand and gravel were used for the aggregate and the water-to-cement ratio including K_2SO_4 was 0.57.

The concrete was directly cast into the stainless tube. After casting, the specimens were subjected to heat-curing following a similar curing cycle to the uni-axial restraint test (see Section 2.1): starting from four hours after casting, heat the specimen to 90 °C at a rate of +35.4 °C/h, maintain for 12 h, then cool to 20 °C at a rate of -34.9 °C/h.

A3.1.2 Expansion test

After heat curing, the specimens were subjected to an expansion test in which the specimens were immersed for 378 days in water kept at 20 °C. It should be noted that the stress-free specimen was wrapped by waterproof aluminum tape with acyl adhesion to maintain the same moisture conditions as the restraint specimens.

The length changes of the concrete in the axial direction (length of 200 mm) were measured by a linear gauge with a precision of 0.0005 mm. The studs for the measurement were installed on the end surfaces in the longitudinal direction of the cylindrical specimen. Strains along the axial and circumferential directions of the stainless tube were also measured by strain gauges (length of 5 mm) attached to the center of the stainless tube. Initial measurements were performed at twenty-four hours after casting.

A3.2 Results and discussion

A3.2.1 Expansion measured from the concrete

The concrete expansions due to DEF in the longitudinal direction are illustrated in Figure A5. Error bars in the figure are the standard deviations of the measured expansions. In the stress-free condition, the onset of expansion was around 20 days and the expansion exceeded 0.5% at 115 days. Finally, the expansion was 0.78% at 378 days. When the concrete was restrained by the thin stainless tube, the longitudinal expansion of t0.25, t0.05, and t0.10 reduced to 0.36%, 0.19%, and 0.23%, respectively. While the longitudinal expansion was reduced by the stainless tube, the reduction was not significant at approximately 24–47% of the stress-free expansion. This is because the expansion in the longitudinal direction was restrained only by friction. The longitudinal expansion of t1.00 was slightly larger than that of t0.50 from 115 days. While this indicates a possible expansion transfer of DEF expansion, this possibility would be rejected due to the reason described in **3.2.2**.

A3.2.2 Strains measured from the stainless tube

Steel tube strains due to DEF in the longitudinal and circumferential directions are illustrated in Figure A6. It is found that DEF expansion is nearly isotropic, so the circumferential strain can be compared with the longitudinal expansion of the stress-free concrete. The circumferential expansion (Figure A6(b)) was drastically reduced in the presence of the stainless tube. All the cases demonstrated an expansion 10% less than that of the stress-free case. For "t1.00", the expansion was only 2% of the stress-free expansion. The longitudinal strain of the stainless tube was within 0.015% and 0.031%: the expansive pressure of concrete is transferred to the stainless tube by means of friction, so the strain is quite small. This is the reason that the concrete specimens were regarded as essentially being in a bi-axial restraint condition. Indeed, slip-like behaviors of the longitudinal strains can be observed in Figure A6. In Figure A5, the longitudinal expansion of t1.00 was slightly larger than that of t0.50. This tendency might be explained by the friction. The longitudinal tube strain of t0.50 was two to three times higher than t1.00, suggestive of larger friction forces acting on the concrete, in which greater friction reduces the longitudinal expansion. Additionally, expansions in the longitudinal and circumferential directions were reduced in the presence of the stainless tube, leading to a significant reduction in volumetric expansion. Therefore, it can be concluded that expansion transfer would not be observed even in the presence of the bi-axial restraint.

The relationship between the longitudinal expansion of the concrete and the circumferential strain is shown in Figure A7. A similar tendency was found for the bi-axial restraint condition, in that the circumferential tube strain is significantly lower than the longitudinal expansion of the concrete. The ratios of the circumferential tube strain to the longitudinal expansion of the concrete are 0.05–0.23, which are similar to those observed in the uni-axial restraint test.

Expansive pressure as a function of *As*/*Ac* is illustrated in Figure A8, which includes the uni-axial restraint data presented in Figure 16. Expansive pressure was calculated from the circumferential strain based on the elastic mechanical model [13, 34]. In this calculation, creep, damage (reduction in Young's modulus), and expansion transfer were not considered. The Young's modulus of the concrete and stainless tube was 35.0 GPa (rough estimation) and 193 GPa (from a material test result), respectively. At 378 days, the calculated expansive pressure, as well as the confinement pressure from the stainless tube, in the circumferential direction for t0.25, t0.50, and t1.00 was 0.76 MPa, 1.12 MPa, and 0.76 MPa, respectively. These results indicate that DEF expansion is quite sensitive to compressive stress. As a result, the bi-axial restraint experiment demonstrated lower expansive pressure. The results of the bi-axial restraint test also suggest that the expansive pressure of DEF concrete under the restraint condition is nearly equal or less than that of ASR concrete.

References

[1] H.F.W. Taylor, C. Famy and K.L. Scrivener: Delayed ettringite formation, Cement and Concrete Research, Vol. 31, pp. 683–693, 2001.

[2] R.J. Flatt and G.W. Scherer: Thermodynamics of crystallization stresses in DEF, Cement and Concrete Research, Vol. 38, pp. 325–336, 2008.

[3] A. Sellier, S. Multon: Chemical modelling of Delayed Ettringite Formation for assessment of affected concrete structures, Cement and Concrete Research, Vol.108, pp. 72–86, 2018.

[4] R.-P. Martin, O. O. Metalssi, F. Toutlemonde: Importance of considering the coupling between transfer properties, alkali leaching and expansion in the modelling of concrete beams affected by internal swelling reactions, Construction and Building Materials, Vol. 49, pp. 23–30, 2013

[5] M. M. Karthik, J. B. Mander, S. Hurlebaus: Deterioration data of a large-scale reinforced concrete specimen with severe ASR/DEF deterioration, Construction and Building Materials, Vol. 124, pp. 20–30, 2013.

[6] O. Omikrine-Metalssi, B. Kchakech, S. Lavaud & B. Godart, A new model for the analysis of the structural/mechanical performance of concrete structures affected by DEF - Case study of an existing viaduct, Structural Concrete, 2016.

[7] H. Bouzabata, S. Multon, A. Sellier, and H. Houari: Effects of restraint on expansion due to delayed ettringite formation, Cement and Concrete Research, Vol. 42, pp. 1024–1031, 2012.

[8] Y. Thiebaut, S. Multon, A.Sellier, L. Lacarrière, L. Boutillon, D. Belili, L. Linger, F. Cussigh, and S. Hadji: Effects of stress on concrete expansion due to delayed ettringite formation, Construction and Building Materials, Vol. 183, pp. 626–641, 2018.

[9] H. Bouzabata, S. Multon, A. Sellier, and H. Houari: Swellings due to alkali-silica reaction and delayed ettringite formation: Characterisation of expansion isotropy and effect of moisture conditions, Cement and Concrete Composites, Vol. 34, pp. 349–356, 2012.

[10] A.E.K. Jones, L.A. Clark: The effects of restraint on ASR expansion of reinforced concrete, Magazine of Concrete Research, Vol. 174, pp. 1–13, 1996.

[11] C. Larive: Apports combinés de l'expérimentation et de la modélisation à la compréhension de l'alcali-réaction et de ses effets mécaniques, Laboratoire Central des Ponts et Chaussées (Edt.), Ouvrage d'Art, Rapport OA 28, 1998

[12] C. Gravel, G. Ballivy, K. Khayat, M. Quirion, M. Lachemi: Expansion of AAR concrete under triaxial stresses: simulation with instrumented concrete block, in: Proc. 11th Int. Conf. Alkali Aggreg. React., Québec, Canada, pp. 949–958, 2000.

[13] S. Multon, F. Toutlemonde: Effect of applied stresses on alkali-silica reaction-induced expansions, Cement and Concrete Research, Vol. 36, pp.912–920, 2006.

[14] C.F. Dunant, K.L. Scrivener: Effects of uniaxial stress on alkali-silica reaction induced expansion of concrete, Cement and Concrete Research, Vol. 42, pp. 567–576, 2012.

[15] M. Berra, G. Faggiani, T. Mangialardi, and A.E. Paolini: Influence of stress restraint on the expansive behaviour of concrete affected by alkali-silica reaction, Cement and Concrete Research, Vol. 40, pp. 1403–1409, 2010.

[16] H. Kagimoto, Y. Yasuda, M. Kawamura: ASR expansion, expansive pressure and cracking in concrete prisms under various degrees of restraint, Cement and Concrete Research, Vol. 59, pp. 1–15, 2014.

[17] B.P. Gautam, D.K. Panesar, S.A. Sheikh, F.J. Vecchio: Multiaxial Expansion-Stress Relationship for Alkali Silica Reaction-Affected Concrete, ACI Materials Journal, Vol. 114, pp.171–184, 2017.

[18] N.W. Hayes, Q. Gui, A. Abd-elssamd, Y. Le Pape, A.B. Giorla, S. Le Pape, E.R. Giannini, Z.J. Ma, L. Charpin, A. Ehrlacher, N.W. Hayes, Q. Gui, A. Abd-elssamd, Y. Le Pape: Monitoring alkali-silica reaction significance in nuclear concrete structural member s, Journal of Advanced Concrete Technology, Vo. 16, pp. 179–189, 2018.

[19] J. Liaudat, I. Carol, C.M. López, V.E. Saouma: ASR expansions in concrete under triaxial confinement, Cement and Concrete Composites, Vol. 86, pp. 160–170, 2018.

[20] S. Kongshaug, O. Oseland, T. Kanstad, M.A.N. Hendriks, E. Rodum, G. Markeset: Experimental investigation of ASR-affected concrete – The influence of uniaxial loading on the evolution of mechanical properties, expansion and damage indices, Construction and Building Materials, Vol. 245, 118384, 2020.

[21] T. U. Mohammed, H. Hamada, and T. Yamaji: Relation between strain on surface and strain over embedded steel bars in ASR affected concrete members, Journal of Advanced Concrete Research, Vol. 1, No. 1, pp. 76–88, 2003.

[22] P. Morenon, S. Multon, A. Sellier, E. Grimal, F. Hamon and E. Bourdarot: Impact of stresses and restraints on ASR expansion, Construction and Building Materials, Vol.140, pp. 58–74, 2017.
[23] M. Kawamura and K. Iwahori: ASR gel composition and expansive pressure in mortar under restraint, Cement and Concrete Composites, Vol. 26, pp. 47–56, 2004.
[24] R.G. Pike: Pressures developed in cement pastes and mortars by the alkali-aggregate reaction, HRB Bulletin, Vol. 172, pp. 34–36, 1967.
[25] C.F. Ferraris, J.R. Clifton, E.J. Garboczi and F.L. Davis: Stress due to alkali-silica reactions in mortars, Mechanisms of Chemical Degradation of Cement-based Systems, K.L. Scrivener and J.F. Young (Eds.), E & FN Spon, pp. 75–82, 1997.
[26] M. Fujii, K. Kobayashi, K. Kojima and H. Mehara: The static and dynamic behavior of reinforced concrete beams with cracking due to alkali–silica reaction, in: Proc. 7th Int. Conf. Alkali Aggreg. React., Ottawa, Canada, pp. 126–130, 1987.
[27] W. Müllauer, R. E. Beddoe, and D. Heinz: Sulfate attack expansion mechanisms, Cement and Concrete Research, Vol. 52, pp. 208–215, 2013.
[28] M. Alnaggar, G. Cusatis, and G. Di Luzio: Lattice Discrete Particle Modeling (LDPM) of Alkali Silica Reaction (ASR) deterioration of concrete structures, Cement and Concrete Composites, Vol. 41, pp. 45–59, 2013.
[29] Badreddine Kchakech: Etude de l'influence de linfluence de l'échauffement subi par un béton sur le risque d'expansions associées à la Réaction Sulfatique Interne, Ph. D thesis of Universite Paris-Est, 2015 (in French)
[30] J. Skalny, V. Johansen, N. Thaulow and A. Palomo: DEF: As a form of sulfate attack, Materiales de Construction, Vol. 46, pp.5–29, 1996
[31] S.G. Hansen and D. Skou: Discussion on "ASR expansion, expansive pressure and cracking in concrete prisms under various degrees of restraint", Cement and Concrete Composites, Vol. 79, pp. 419–421, 2016.

[32] H. Kagimoto, Y. Yasuda and M. Kawamura: Reply to the discussion by S.G. Hansen of the paper "ASR expansion, expansive pressure and cracking in concrete prisms under various degrees of restraint", Cement and Concrete Composites, Vol. 79, pp. 422–423, 2016.

[33] T. Miura, H. Nakamura and Y. Yamamoto: Impact of origination of expansion on three-dimensional expansion crack propagation process due to DEF evaluated by mesoscale discrete model, Construction and Building Materials, Vol. 260, 119911, 2020.

[34] Y. Kawabata, J.-F. Seignol, R.-P. Martin and F. Toutlemonde: Macroscopic chemo-mechanical modeling of alkali-silica reaction of concrete under stresses, Construction and Building Materials, Vol. 137, pp. 234–145, 2017.

Table 1 Summary of experimental conditions in previous studies related to expansive pressure.

	Bouzabata et al. [7]		Thiebaut et al. [8]		Müllauer et al. [27]				
Mortar/Concrete	Mortar		Concrete		Mortar (two cements)				
Specimen size	40 × 40 × 160 mm		100 × 100 × 500 mm		φ30 × t2.5 × L70 mm (thin wall)				
Expansion mechanism	DEF, no ESA		DEF, no ESA		ESA under Na_2SO_4 solution (SO_4^{2-}: 1.5 & 30 g/L)				
Longitudinal direction									
Restraint condition	External restraint by four threaded stainless steel bars		Internal restraint by a stainless steel bar with interfacial bonding		Internal restraint by a stainless steel bar without interfacial bonding				
As/*Ac* (%)	0.8	4.9	1.1	1.1	3.3	5.8	9.1	13.1	17.8
Transverse direction									
Restraint condition	No restraint		No restraint	Stirrup	No restraint				
As/*Ac* (%)	–	–	–	0.7	–				
Method to measure/estimate expansive pressure	Estimation from mortar surface strain		Estimation from concrete surface strain		Estimation from deformation of the specimen				
Expansive pressure (MPa, longitudinal direction)	1.6	4.2	5.8	5.4	7.2–8.7	7.0–7.9	6.7–7.6	7.6–7.9	7.9–9.4

Table 2 Mixture proportion of the concrete.

Unit content (kg/m^3)				
Water	Cement	Sand	Gravel	K_2SO_4
173	337	798	965	18.85

Table 3 Chemical composition of the cement.

Chemical composition (%)												
LOI	SiO_2	Al_2O_3	Fe_2O_3	CaO	MgO	SO_3	Na_2O	K_2O	TiO_2	P_2O_5	MnO	SrO
1.15	20.16	5.05	2.52	65.00	1.35	3.04	0.26	0.36	0.31	0.65	0.07	0.05

Table 4 Mineral composition of the cement by Bogue equation.

Mineral composition (%)			
C_3S	C_2S	C_3A	C_4AF
65.1	20.16	5.05	2.52

Table 5 Estimated imposed strains (positive in tension/expansion).

	measurement				estimation			
	ε_{free} (%)	ε_{res} (%)	ε_{e} (%)	σ_{DEF} (MPa)	E_c (GPa)	ε_{cr} (%)	ε_{imp} (%)	$\varepsilon_{imp}/\varepsilon_{free}$ (%)
Free	2.11	-	-	-	-	-	-	-
ϕ9.2	-	0.38	-0.02	-1.98	8.6	-0.05	0.45	0.21
ϕ13	-	0.39	-0.03	-2.44	8.7	-0.06	0.47	0.22
ϕ17	-	0.29	-0.03	-2.92	10.8	-0.05	0.37	0.17
ϕ26	-	0.27	-0.03	-2.69	10.0	-0.05	0.35	0.17

ε_{free}: stress-free expansion (%), σ_{DEF}: expansive pressure measured by the load cell (MPa)

Table A1 Mixture proportion of the concrete for the bi-axial restraint test.

Unit content (kg/m^3)				
Water	Cement	Sand	Gravel	K_2SO_4
174	290	835	973	14.5

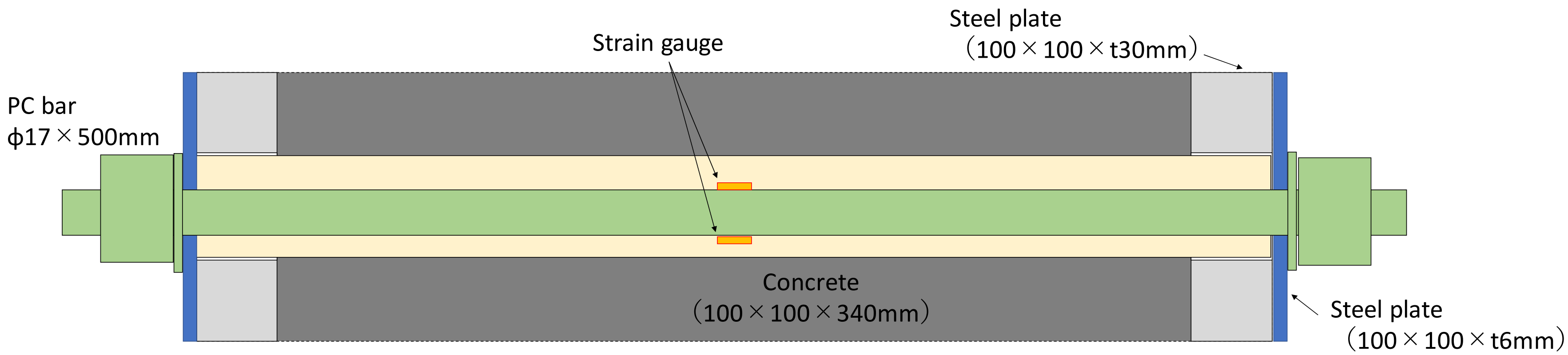

(a) Specimen without a load cell

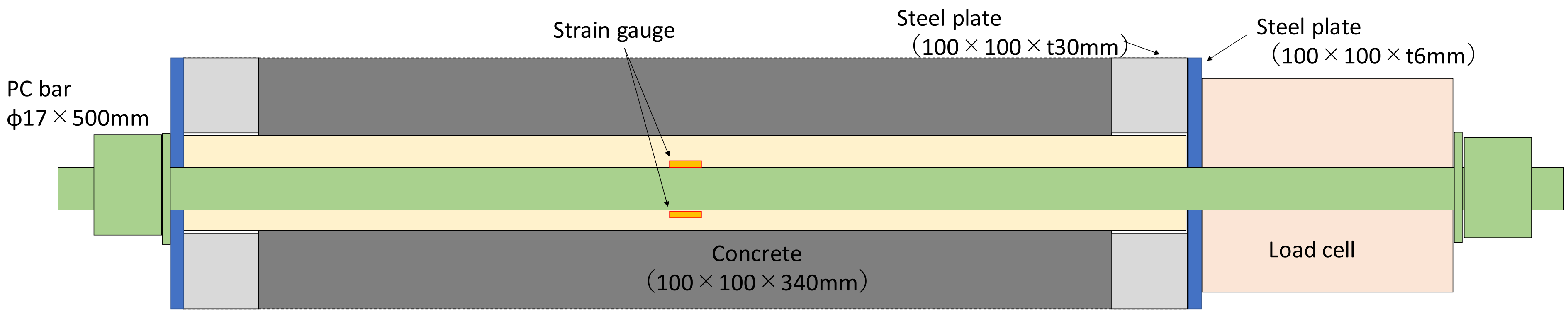

(b) Specimen with a load cell

Figure 1 Apparatus for the expansion test.

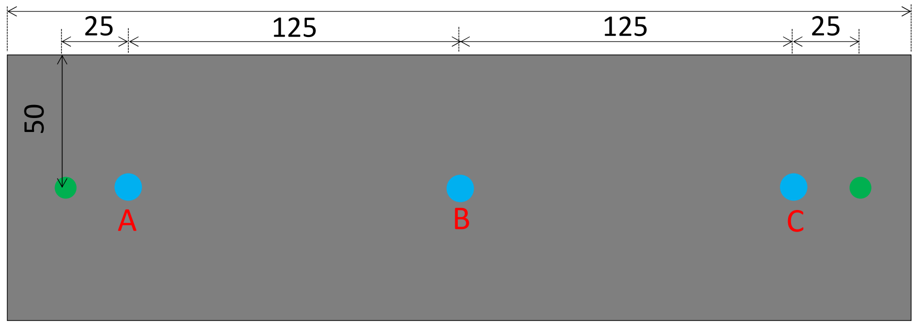

(a) Front view

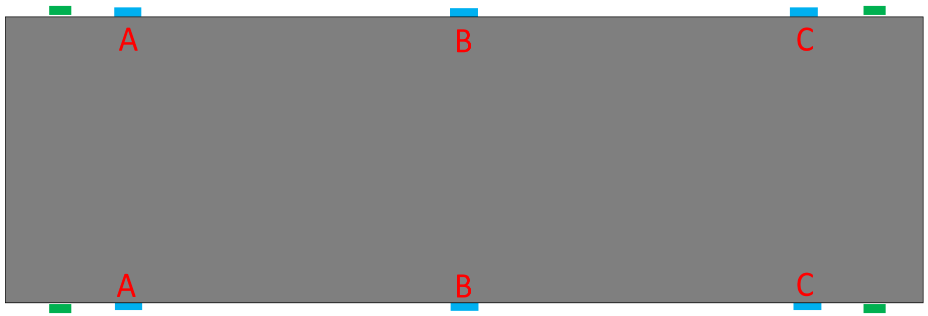

(b) Lateral view

Figure 2 Measurement points on the test specimens (green points denote the location of studs for measuring longitudinal expansion while blue points are for transversal expansion).

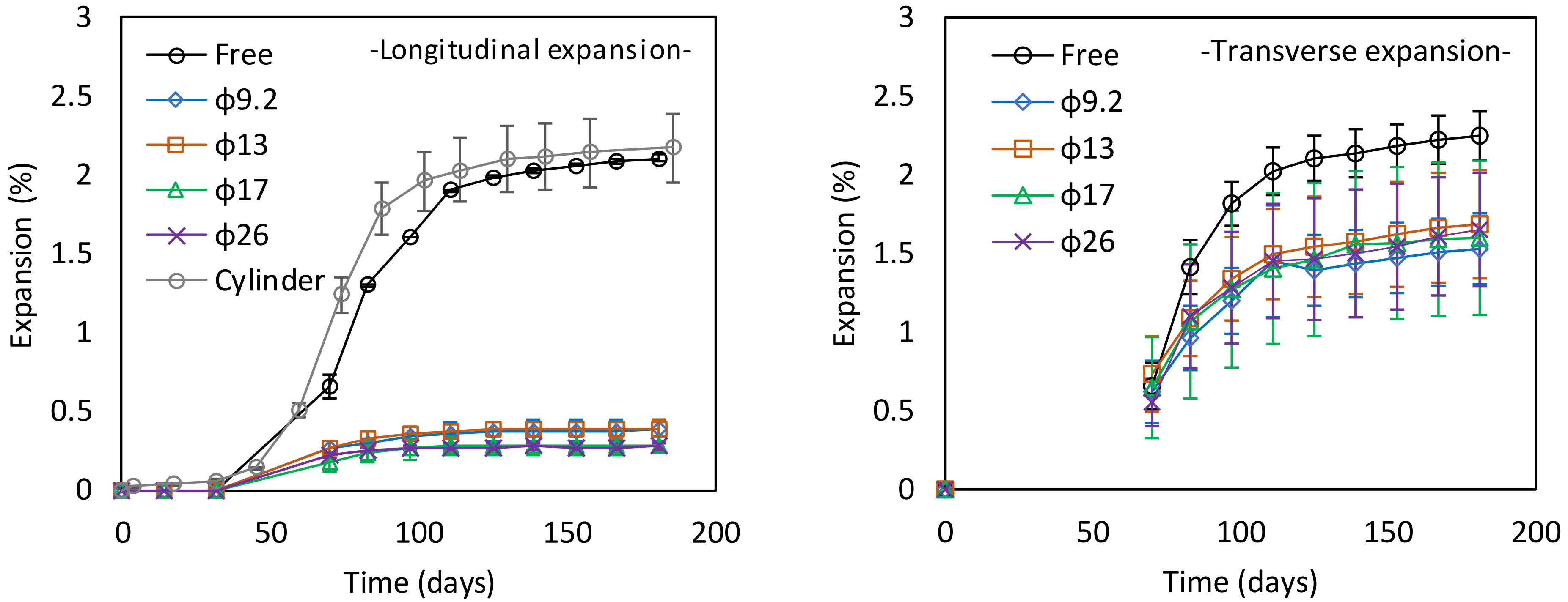

(a) Longitudinal expansion **(b) Transverse expansion**

Figure 3 Expansion of the concrete. Error bars indicate the standard deviation.

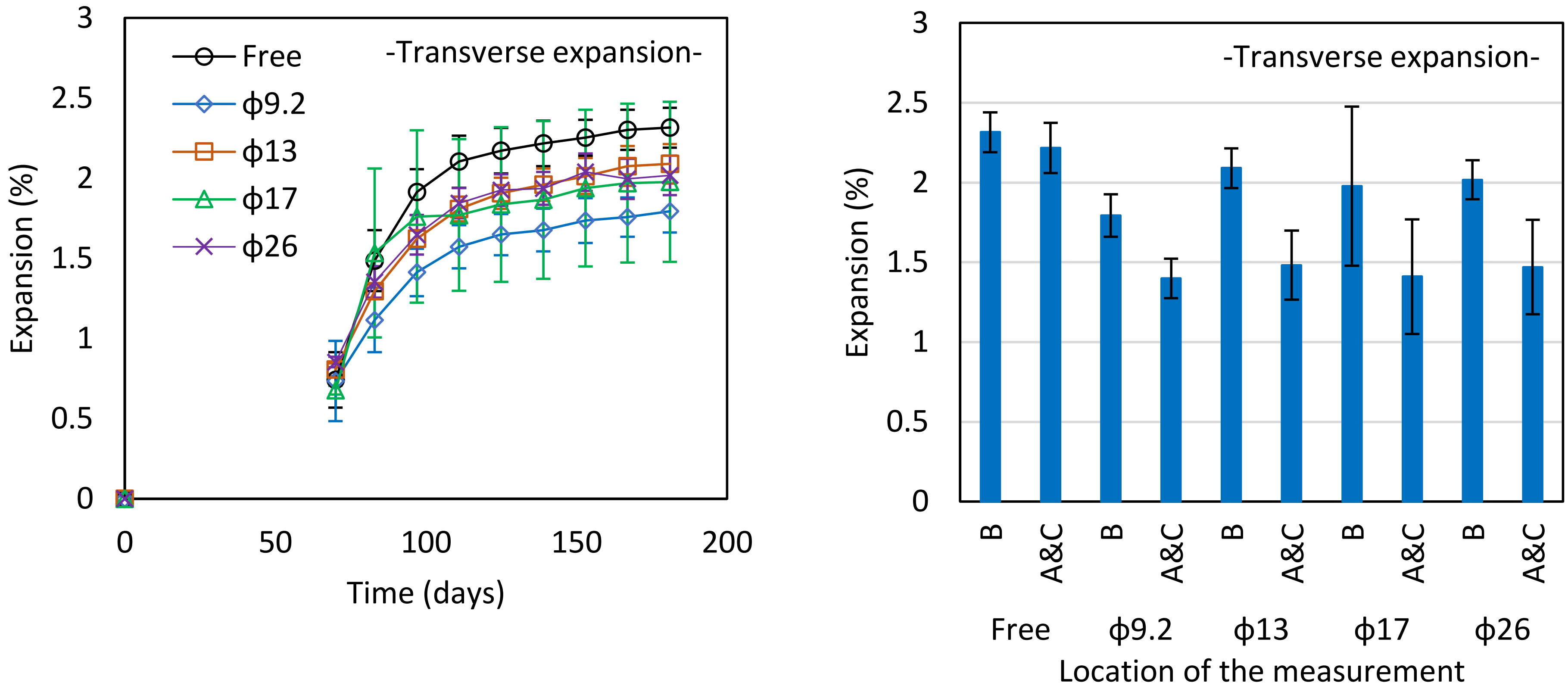

(a) Transverse expansion at point B

(b) Transverse expansion at 181 days

Figure 4 Transverse expansion of the concrete at different locations. Point B was at the center of the longitudinal direction and A and C were at 150 mm from the center. These locations are illustrated in Figure 2.

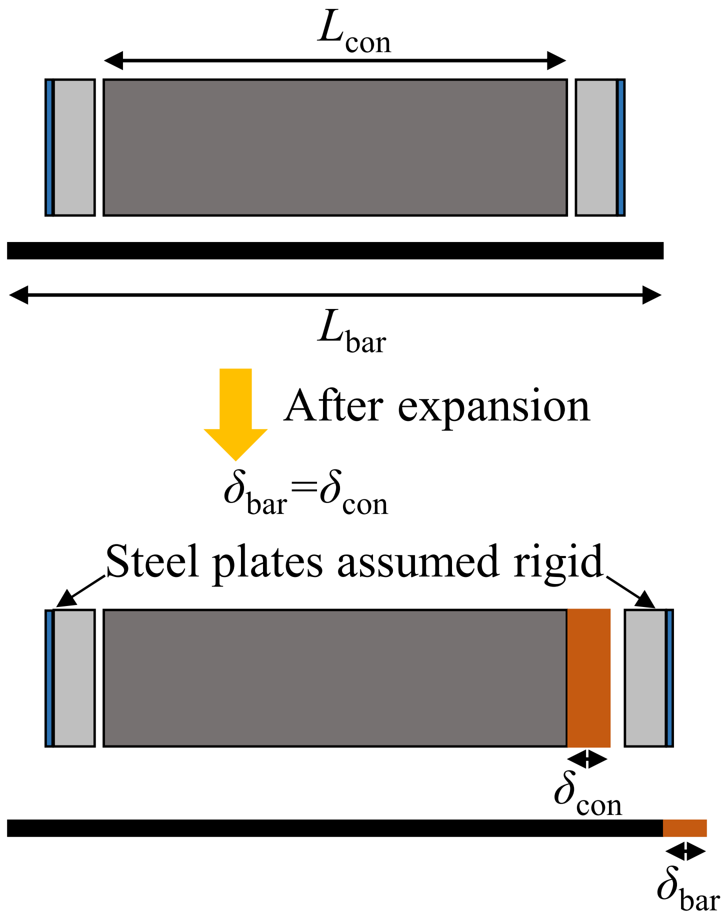

Figure 5 Schematic diagram for the calibration of the steel bar strain.

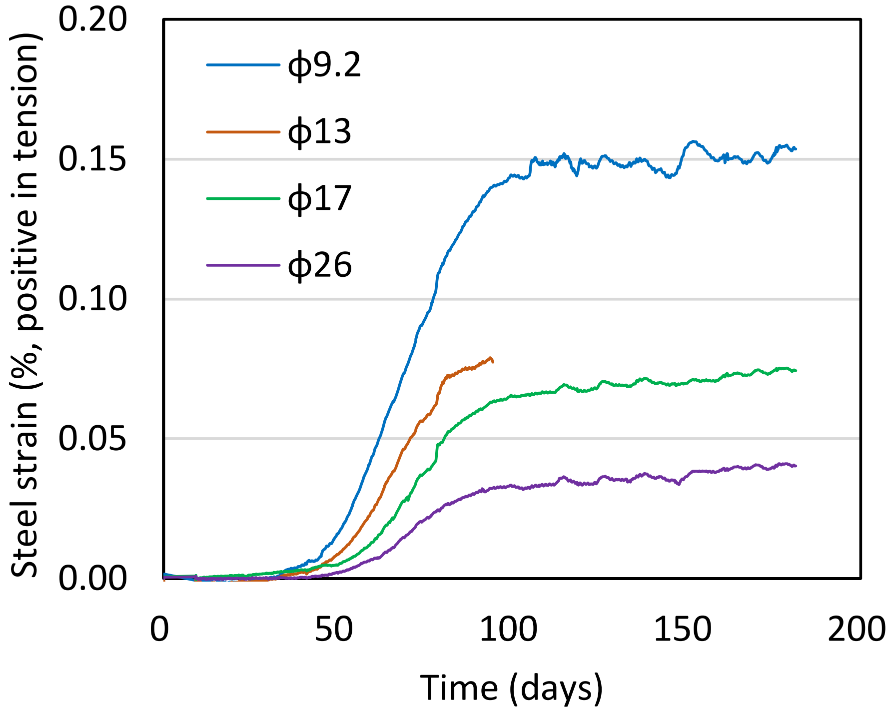

Figure 6 Strain of the steel bar as measured after steel bar strain calibration.

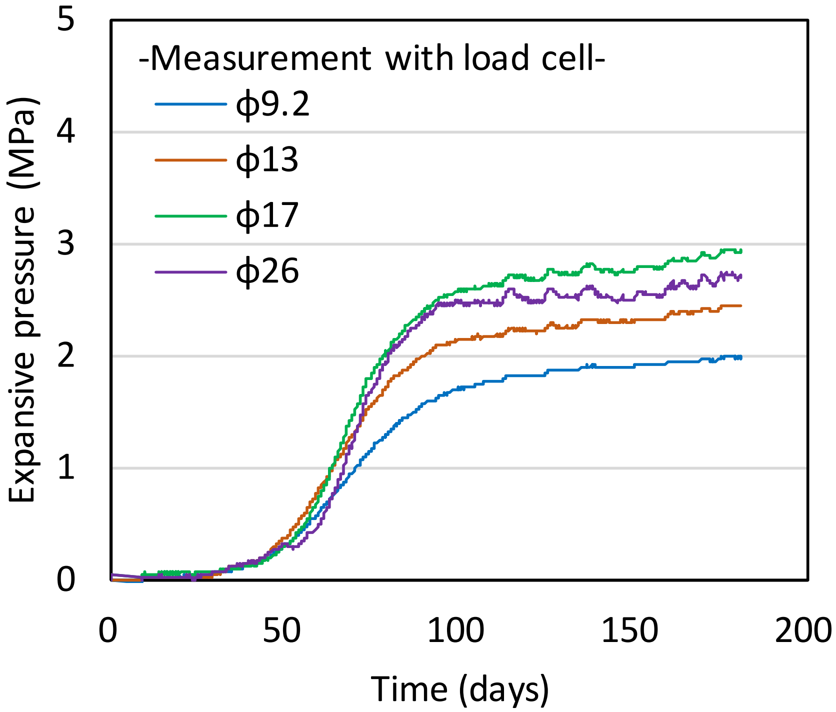

Figure 7 Expansive pressure measured by the load cell (direct measurement).

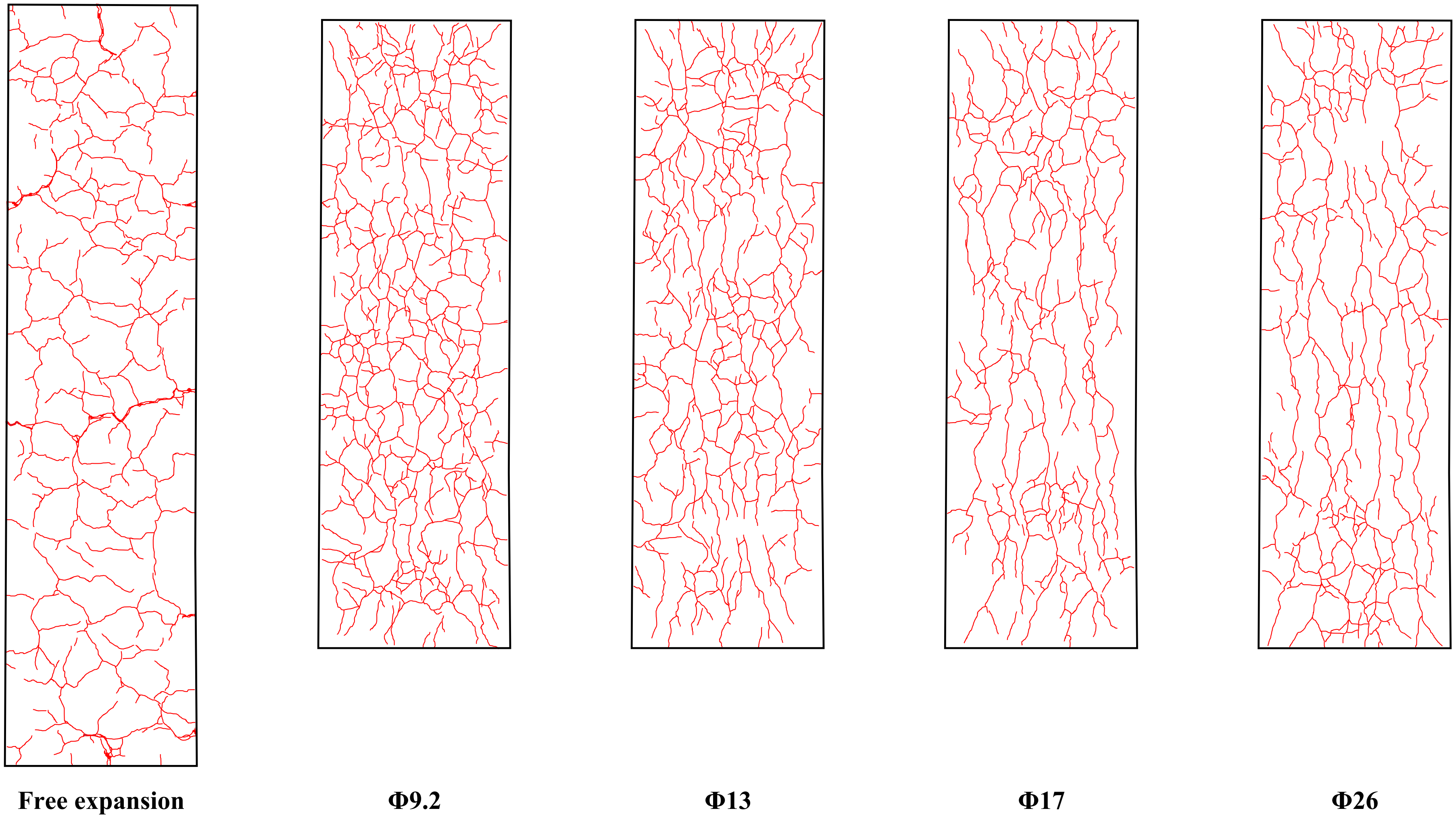

Figure 8 Surface crack patterns of the concrete specimens at 181 days. Note that the length of the stress-free and restrained specimens were 400 mm and 340 mm, respectively.

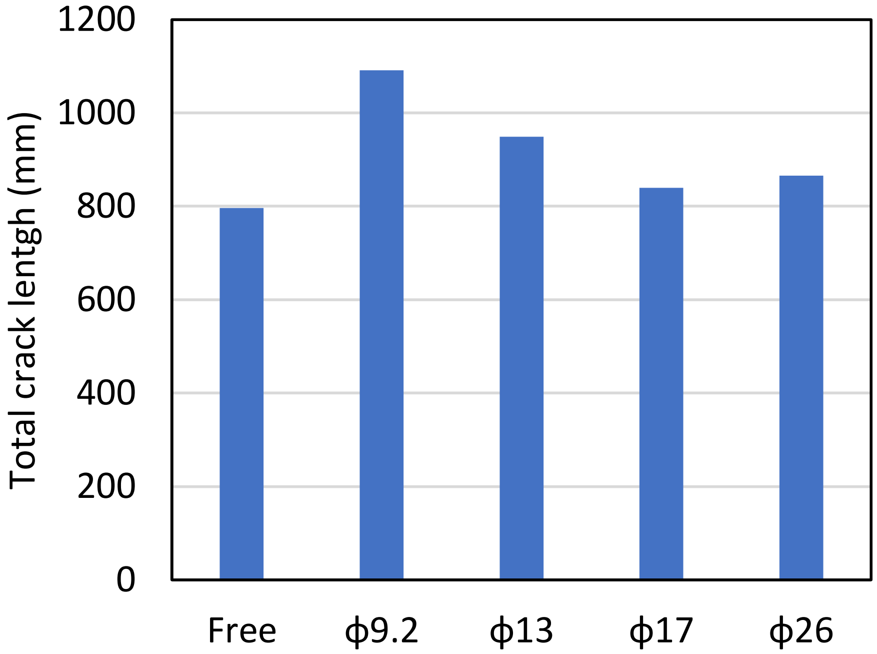

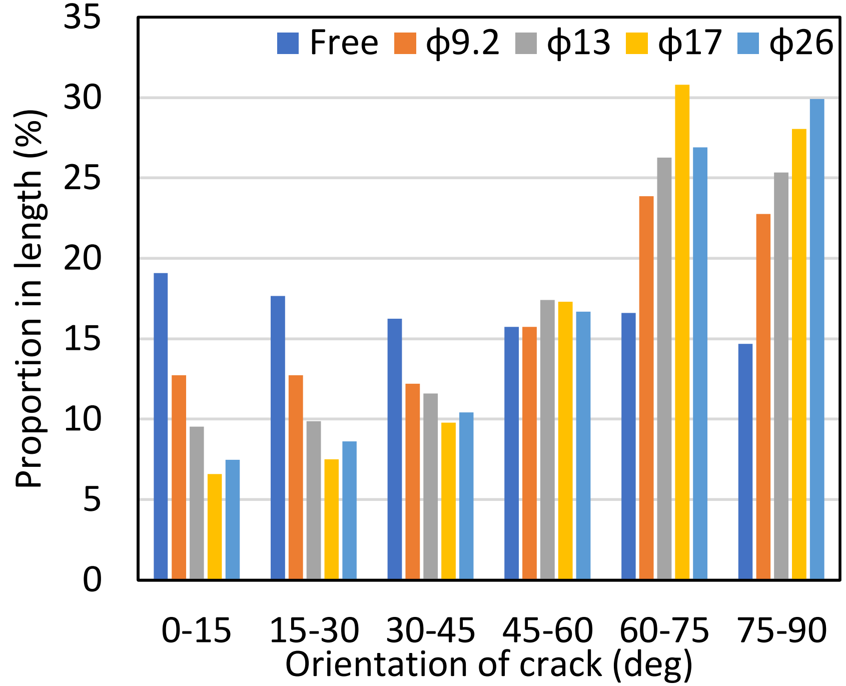

(a) Total length

(b) Crack orientation

42 **Figure 9 Total length and orientation of the surface cracks. Note that the orientation of crack of 90 (deg.) corresponds to the longitudinal**

43 **direction whilst 0 (deg.) corresponds to the transverse direction.**

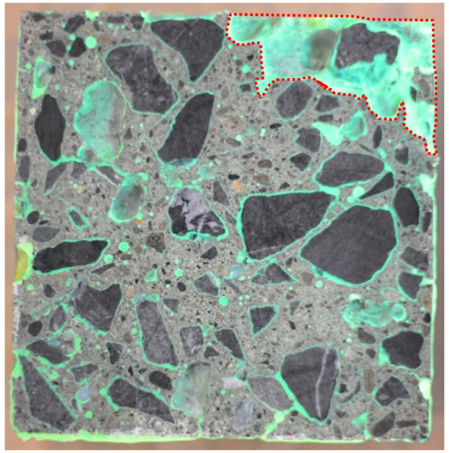

Free expansion

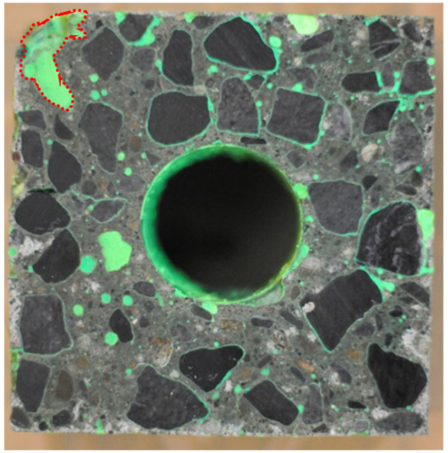

Φ9.2

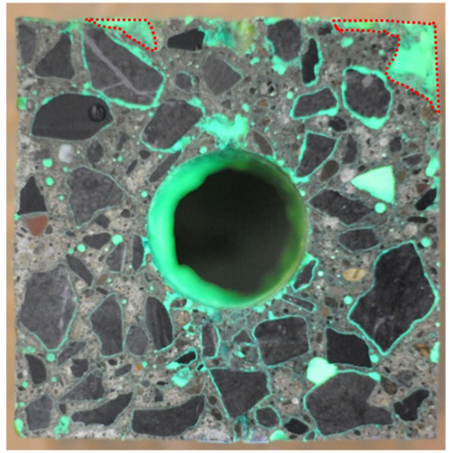

Φ13

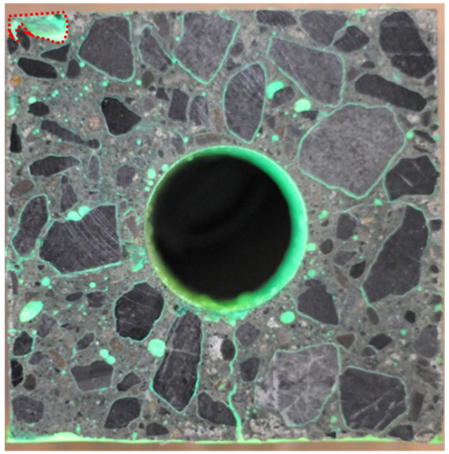

Φ17

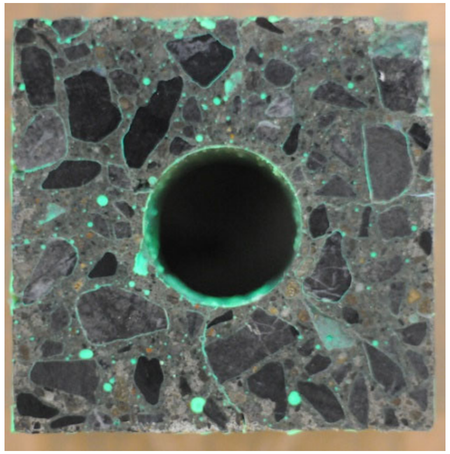

Φ26

Figure 10 Internal crack pattern in the transverse direction.

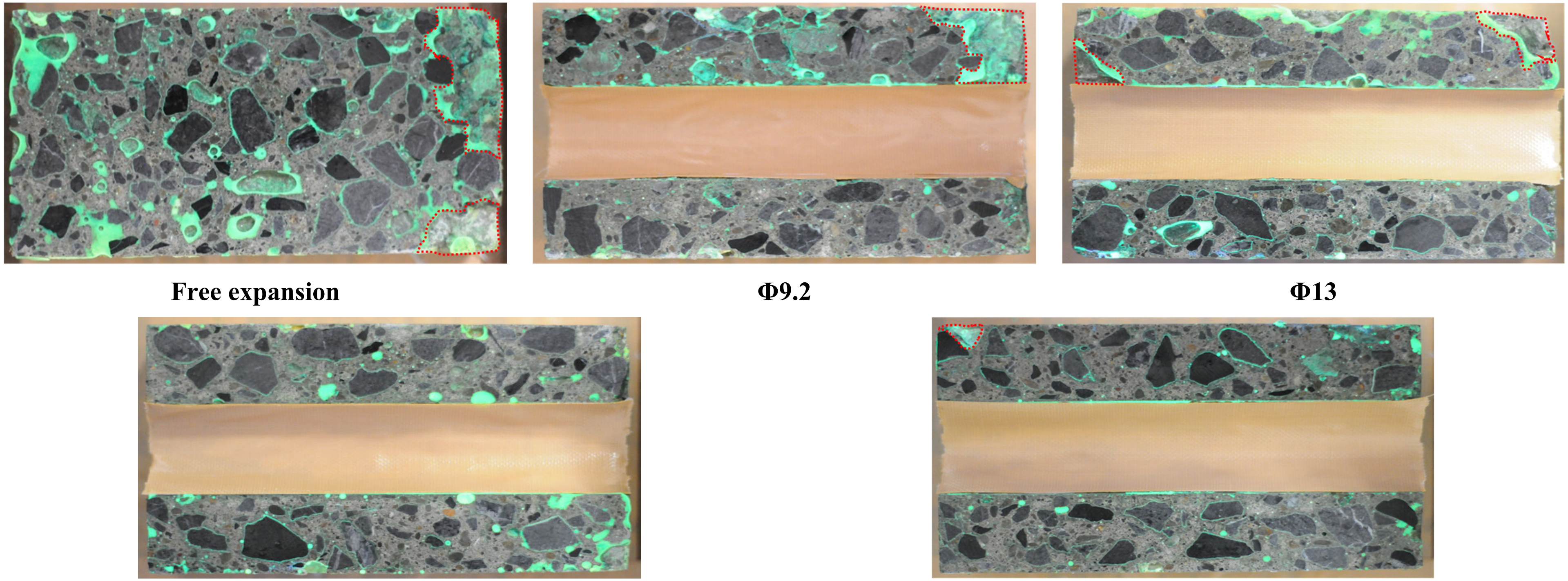

Figure 11 Internal crack pattern in the longitudinal direction.

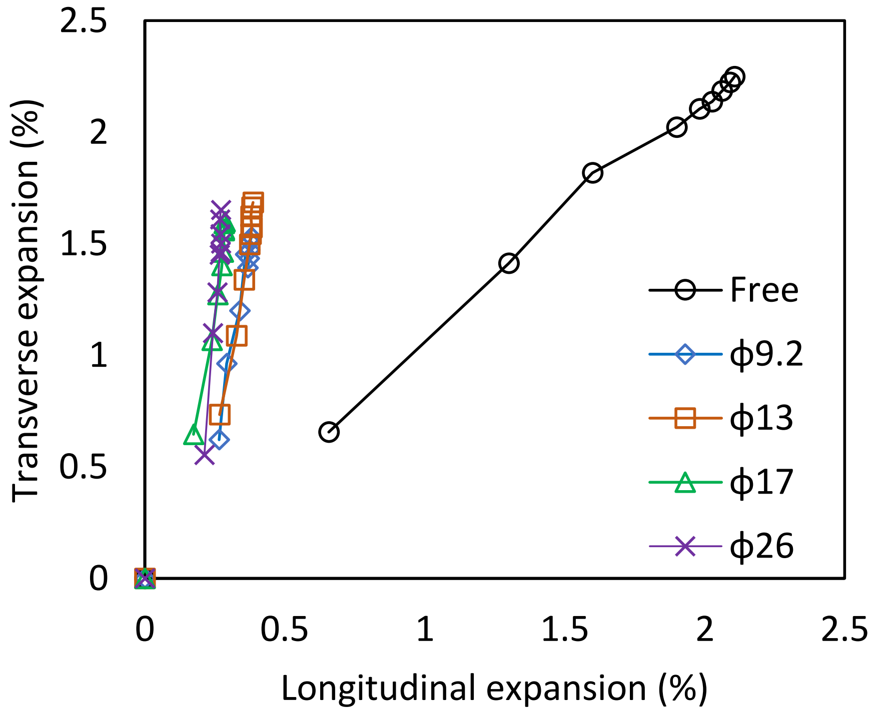

Figure 12 Longitudinal expansion vs. the transverse expansion of the concrete.

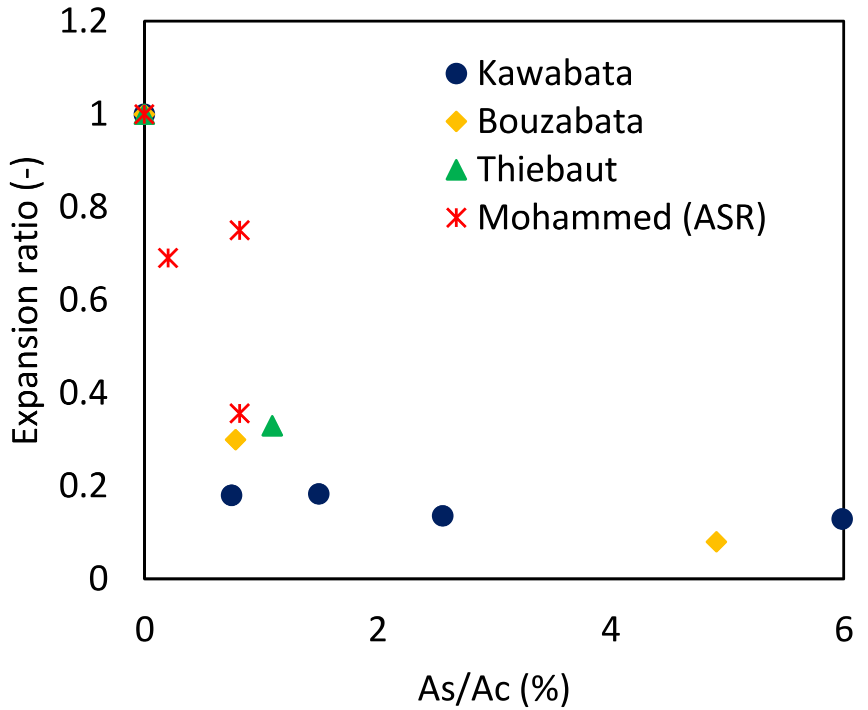

Figure 13 ***As*****/*****Ac*** **vs. the expansion ratio.**

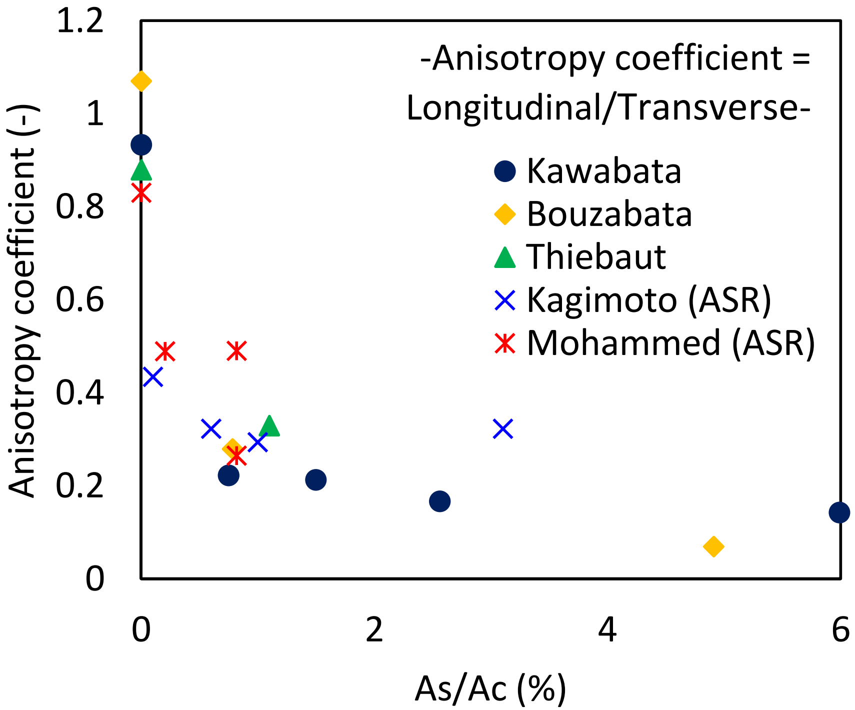

Figure 14 ***As/Ac*** **vs. the anisotropy coefficient**.

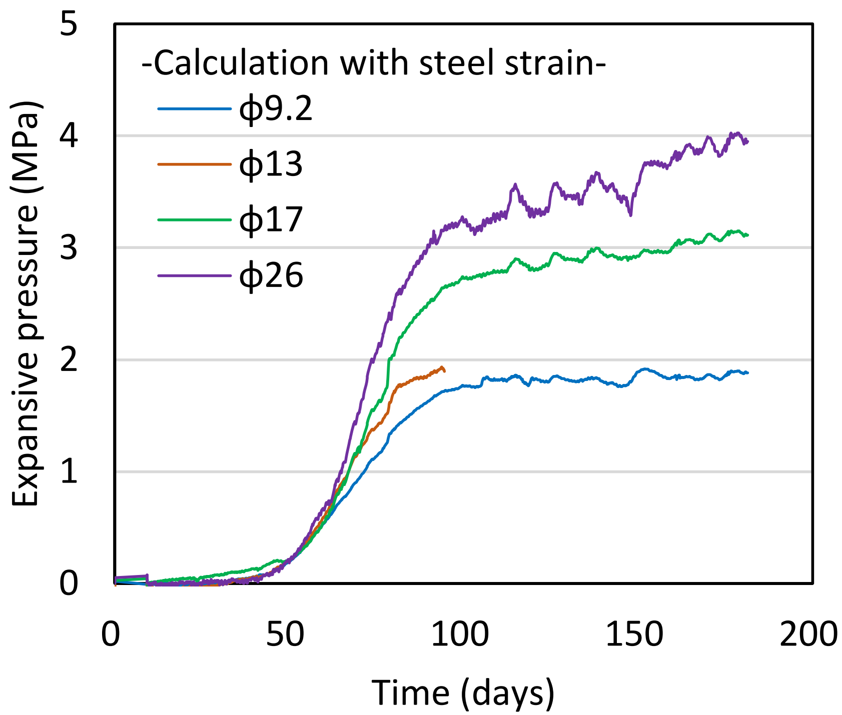

Figure 15 Expansive pressure calculated using the uncalibrated steel bar strain.

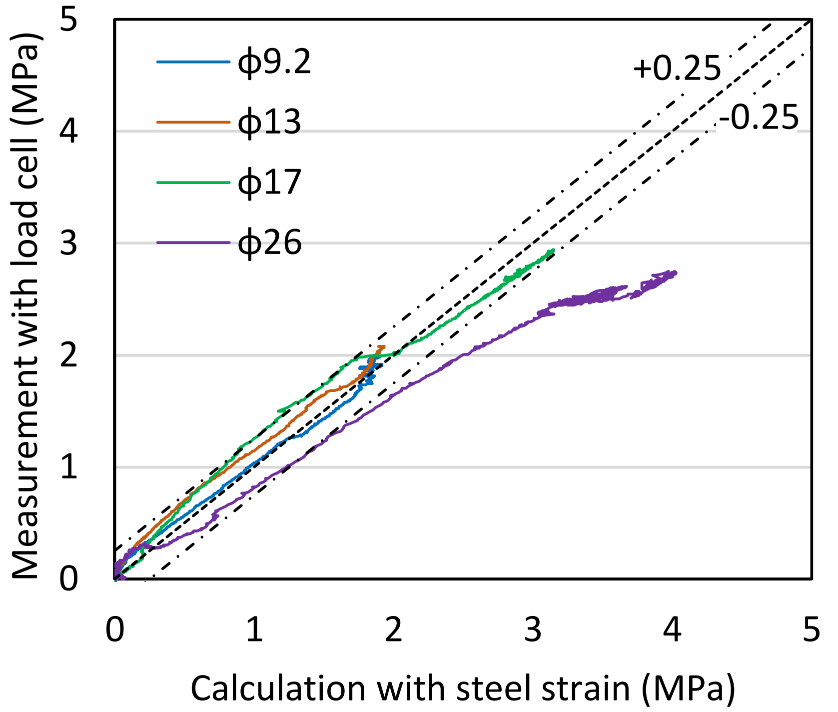

Figure 16 Expansive pressure from the steel strain vs. the load cell measurement results.

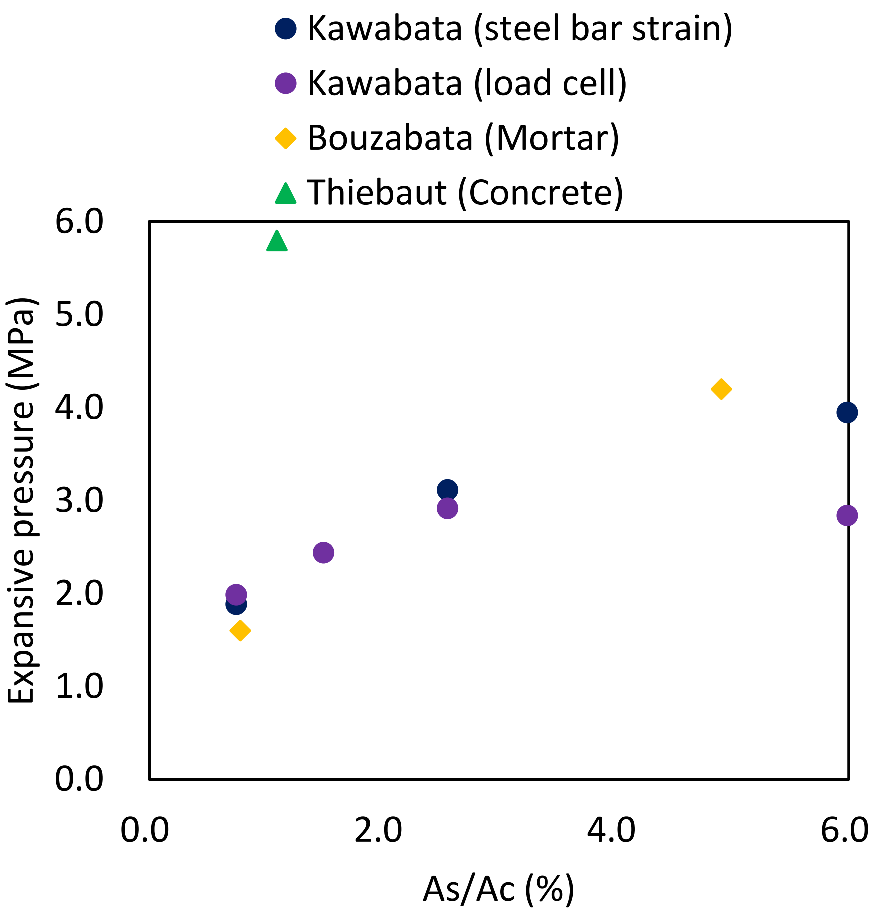

Figure 17 ***As*/*Ac* vs. expansive pressure. The method used to calculate or measure the expansive pressure is described in parentheses.**

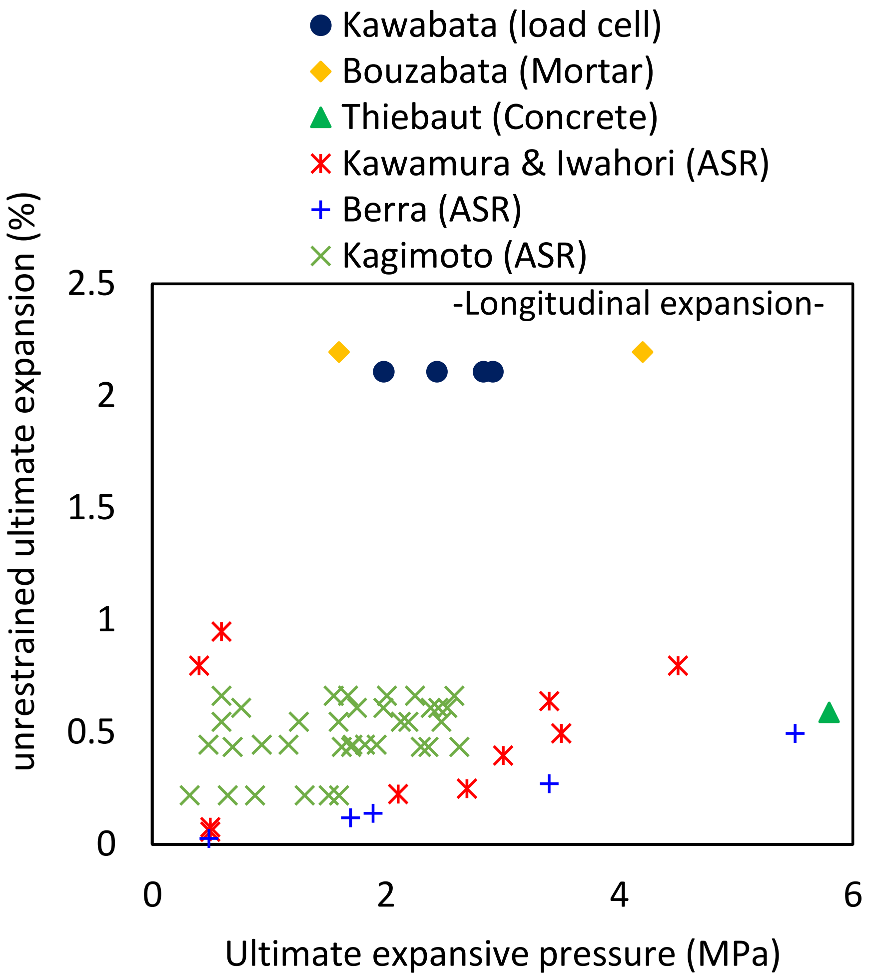

Figure 18 Ultimate expansive pressure vs. unrestrained/free ultimate expansion.

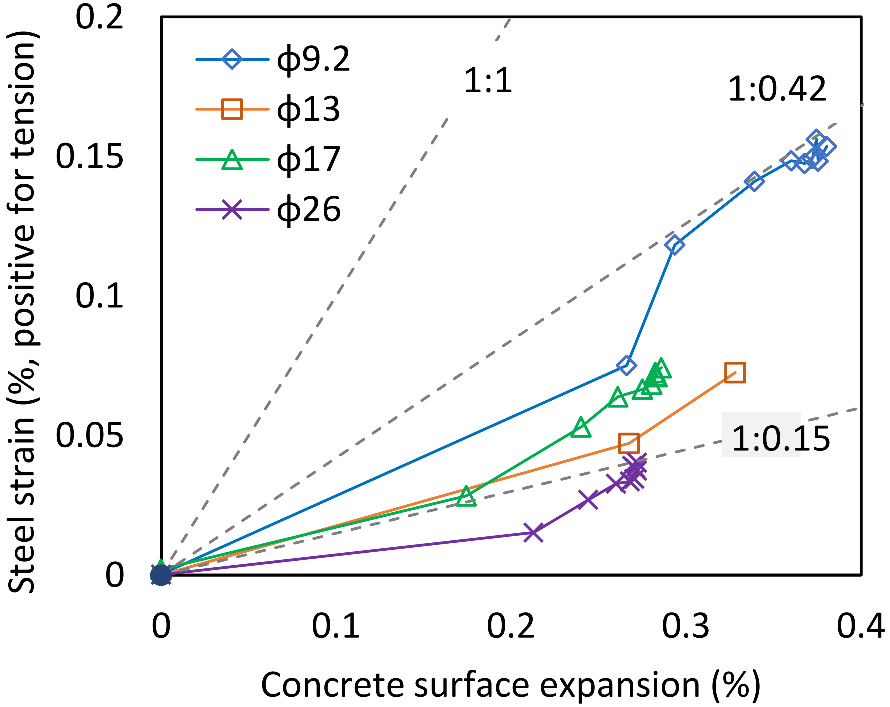

Figure 19 Concrete surface expansion vs. calibrated longitudinal steel strain.

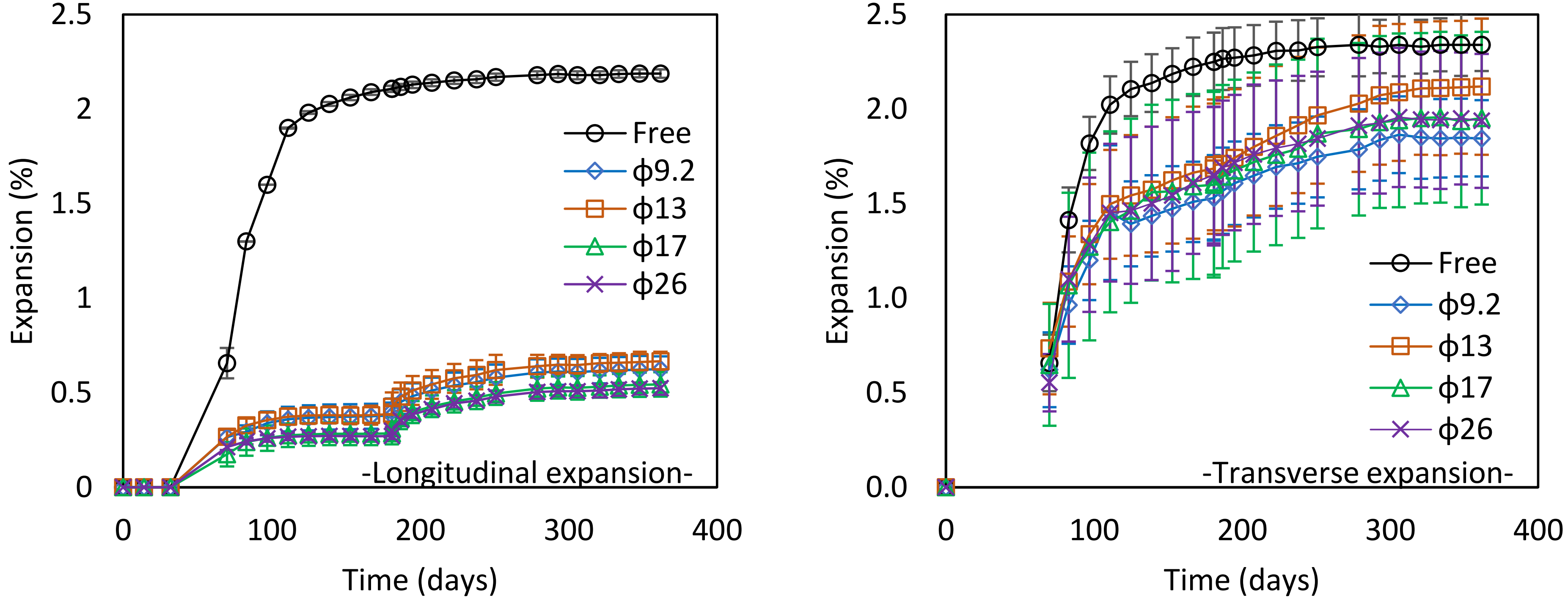

(a) Longitudinal expansion **(b) Transverse expansion**

Figure A1 Expansion of the concrete including releasing the restraint at 181 days.

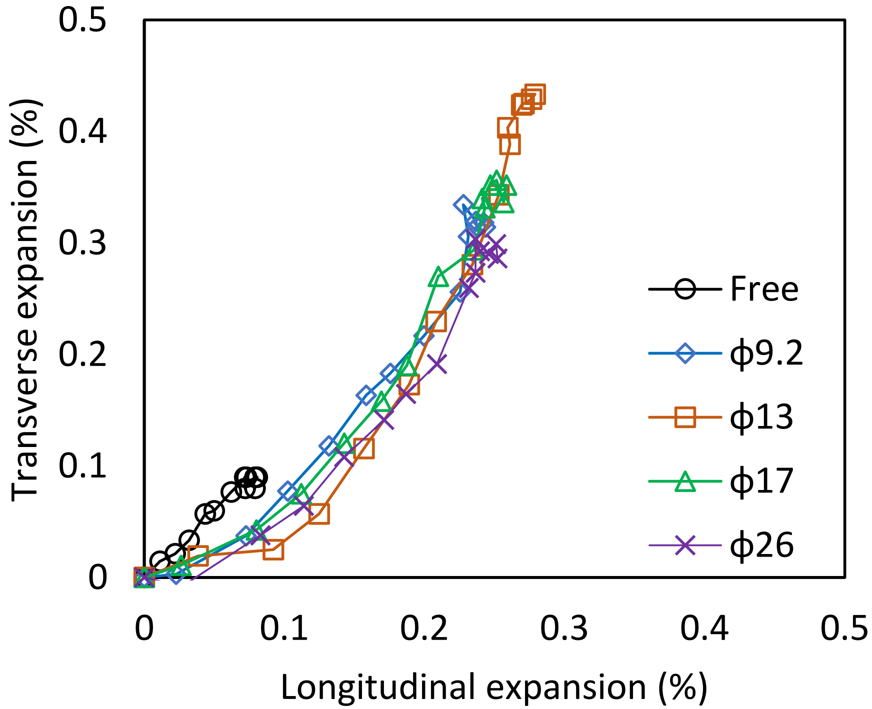

Figure A2 Longitudinal expansion vs. transverse expansion after releasing the restraint. The expansion of the concrete after releasing the restraint is normalized by subtracting the final expansion before restraint release.

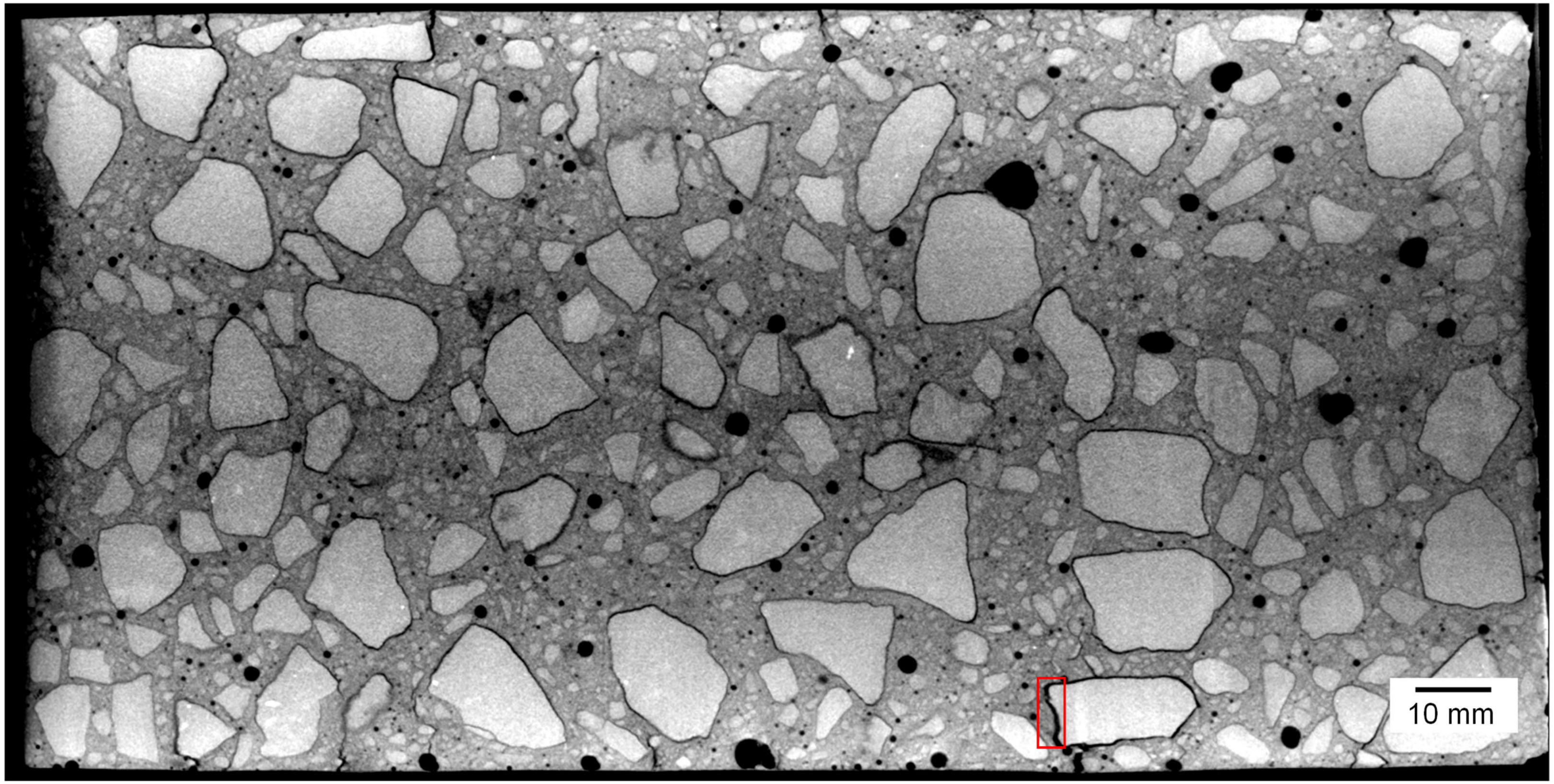

Figure A3 X-ray CT image of the concrete cylindrical specimen. The red rectangle shows the gap with a 0.9-mm width.

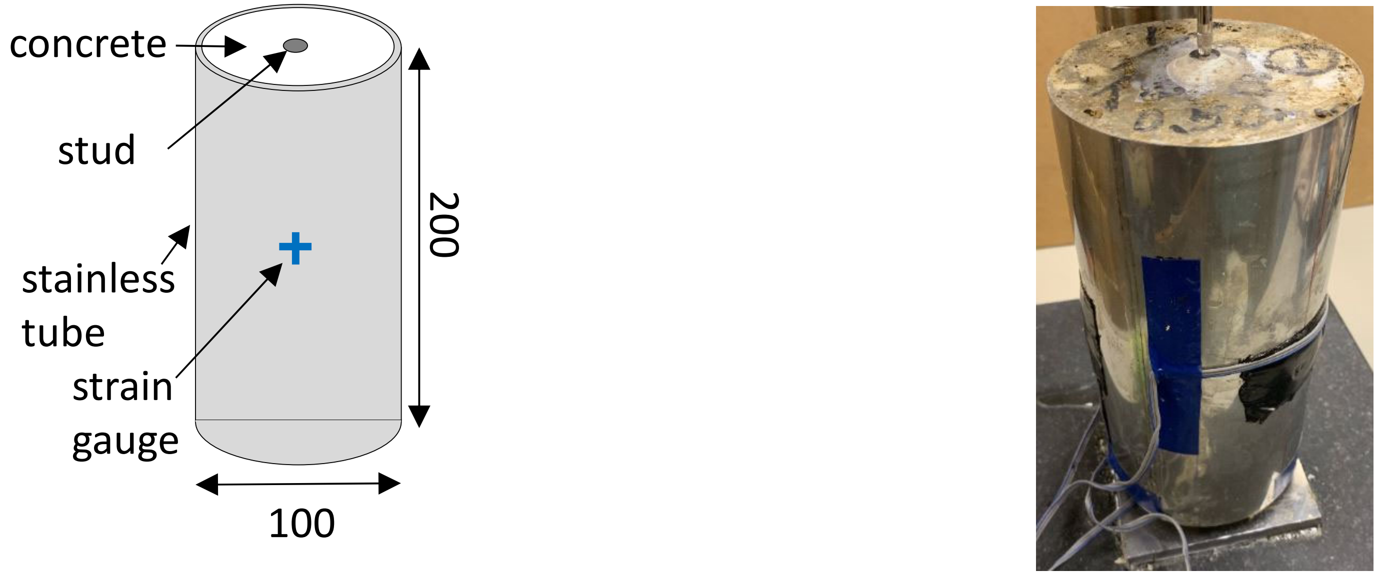

(a) Specimen details **(b) Photo**

Figure A4 Test specimen for the bi-axial restraint.

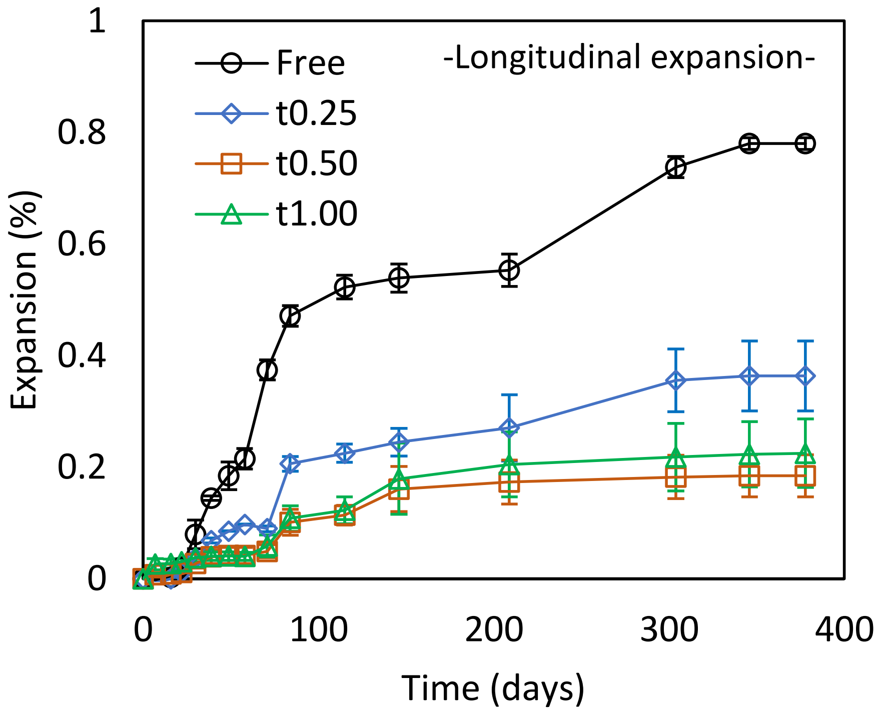

Figure A5 Longitudinal expansion of the cylindrical concrete specimen (bi-axial restraint case).

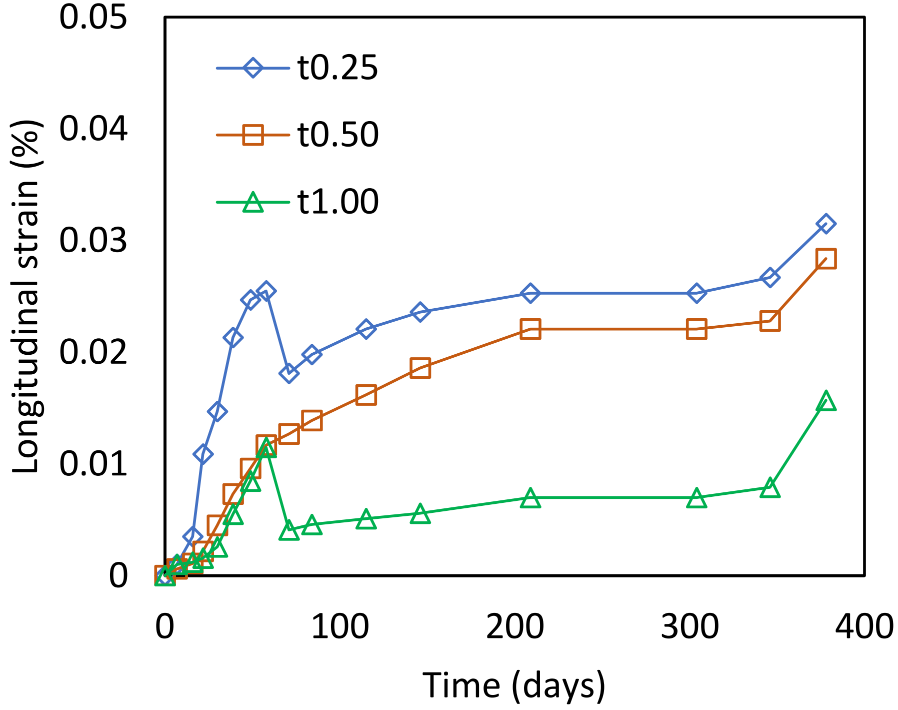

(a) Longitudinal strain

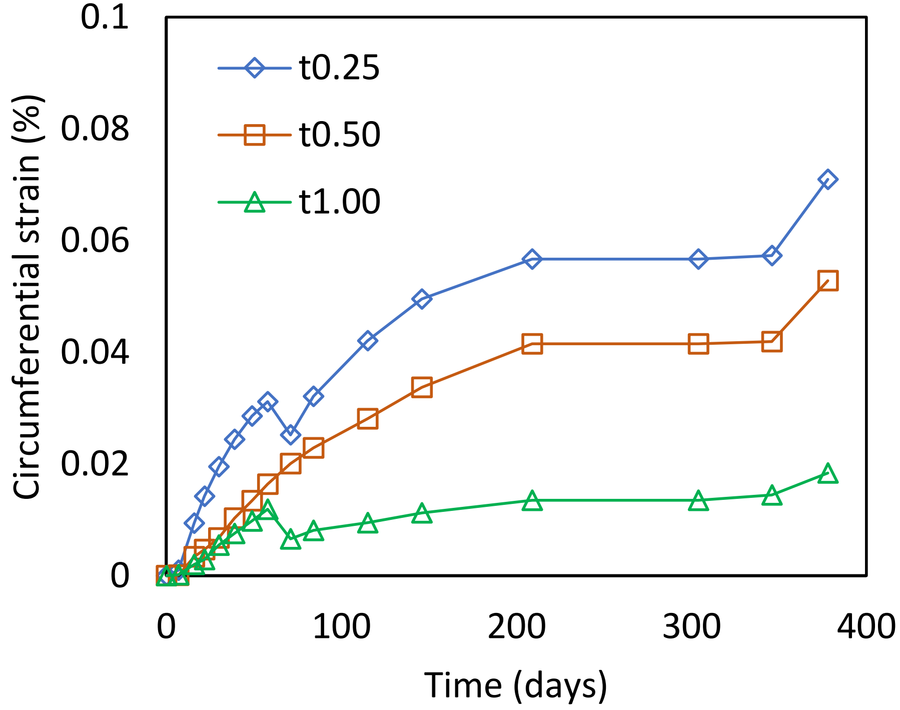

(b) Circumferential strain

Figure A6 Longitudinal and circumferential strains of the stainless tube (bi-axial restraint case).

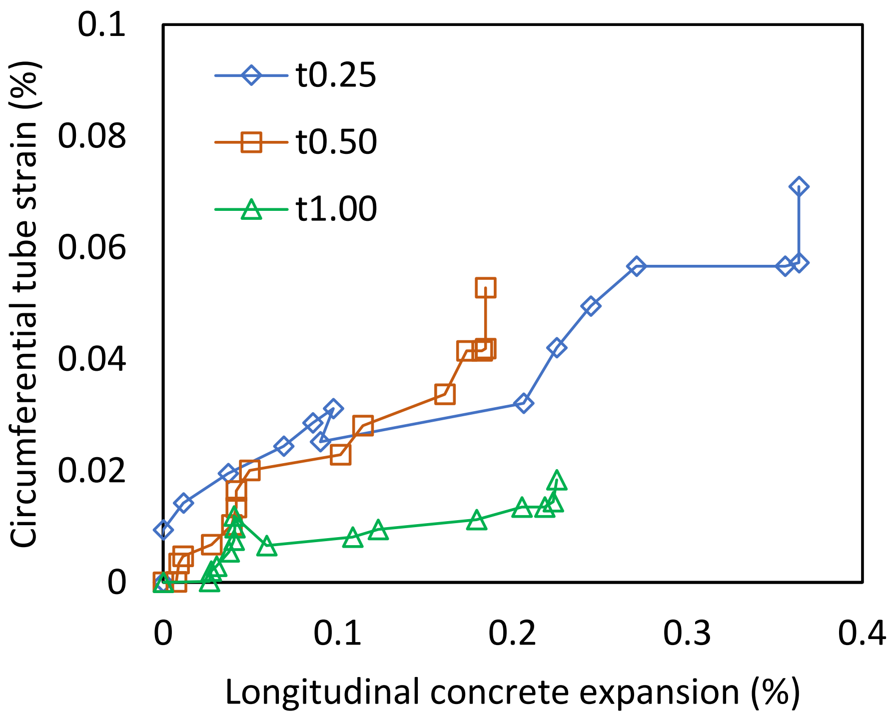

102

103 **Figure A7 Longitudinal expansion of the concrete vs. circumferential strain (bi-axial restraint case).**

104

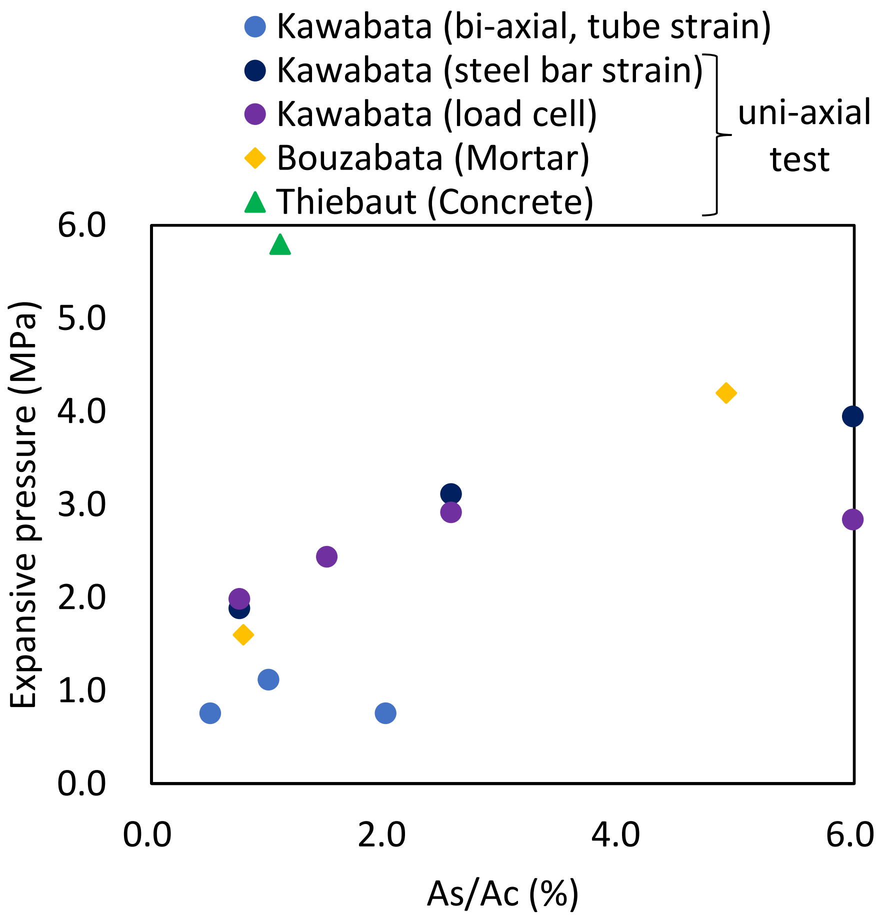

Figure A8 ***As/Ac*** **vs. expansive pressure.**